中国激光

基于超材料的太赫兹光电导天线

谷建强[1*]，王可蒙[1]，许祎[1]，欧阳春梅[1]，田震[1]，韩家广[1]，张伟力[2]

[1]天津大学精密仪器与光电子工程学院太赫兹研究中心，天津 300072；

[2]俄克拉荷马州立大学电气与计算机工程学院，俄克拉荷马 静水城 74078，美国

摘要 发展高性能的光电导天线是推动太赫兹科学及其相关技术不断进步的重要手段。系统地介绍了基于金属和介质超材料的高效光电导天线的研究工作，梳理了此类天线的发展历程并展望了其应用前景。关于超材料天线的研究主要是基于两类方法展开的，第一类是利用纳米级金属/介质超材料操控飞秒泵浦激光与光电导天线衬底间的相互作用，第二类方法则是在原有天线结构的基础上设计微米级金属/介质超材料对太赫兹波进行直接操控。这些基于超材料的新方法极大地促进了光电导天线的发展及其在交叉领域的应用。

关键词 太赫兹技术；超快光学；光电导天线；超材料；局域场增强；太赫兹辐射；太赫兹探测

中图分类号 O434 **文献标志码** A **doi**：10.3788/CJL202148.1914004

1 引 言

得益于近四十年来的蓬勃发展，太赫兹科学与技术在材料科学[1-2]、凝聚态物理[3]、安全监测[4-6]、无线通信[7-8]、生物医学[9-12]、药物检测[13]、成像传感[14-17]等研究领域展现出重要的应用价值和良好的发展前景。作为太赫兹技术的基石，太赫兹辐射源和探测器备受研究人员的关注，目前，已被提出的太赫兹辐射和探测机制多达数十种[18-26]，关于太赫兹辐射源和探测器的研究贯穿了整个太赫兹技术的发展历程。近年来太赫兹技术与其他学科愈发紧密地交叉融合，这对太赫兹辐射源的功率、效率、带宽以及探测器的灵敏度、带宽和噪声提出了更严格的要求[27]。由此可见，关于太赫兹辐射源和探测器的研究并未告一段落，而是迈上了一个新的台阶，进入了一个更高层次的发展阶段。

在众多的太赫兹辐射源和探测器中，光电导天线(PCA)的地位是毋庸置疑的，它不仅是最早开发出来的相干辐射源和探测器，而且至今仍在各实验室和商业化太赫兹系统中发光发热。伴随着飞秒激光技术的发展，1975 年，贝尔实验室的 Auston[28] 发明了光电导开关，实现了皮秒级的光电流和电磁脉冲，被视作光电导天线的开端。此后，研究者对光电导天线开展了系列化的研究[18,29-30]，将其打造成辐射和探测太赫兹脉冲的关键器件。特别是在 1990 年，借助光电导天线发射、探测太赫兹波，Grischkowsky 等[30] 首次提出太赫兹时域光谱技术，从此太赫兹时域光谱技术一直是太赫兹波段光谱研究和成分鉴别的主要手段。光电导天线具有高动态、宽频谱的性能以及对泵浦激光要求低、与光纤技术兼容等特点，在商业化太赫兹时域光谱系统中备受青睐。而天线性能不断迭代更新[31-40]，相关研究已涵盖了天线的各个要素，包括半导体衬底[41-45]、天线结构[46-48]、材料材质[49-50]、激光泵浦[51-54]、偏置电压[55-56]和准直透镜[57-60]等多个方面。这些研究有效提升了天线的性能，使天线更加实用化。目前，商业化的光电导天线的带宽已经达到了 7 THz，动态范围高于 100 dB，功率大于 70 μW，噪声功率谱密度低于 10^{-12} V^2/Hz，天线采用全光纤封装，对泵浦激光功率的要求只有 20 mW，对偏置电源的需求只有 10 mW，能满足大多数近距离下低吸收样品的光谱分析需要。但是与固态太赫兹源相比，光电导天线的功率还低至少两个数量级，与低温热探测器相比，探测天线的灵敏度也不足，而且具有

收稿日期：2021-06-15；**修回日期**：2021-07-07；**录用日期**：2021-07-19

基金项目：国家自然科学基金(61975143，61622505，61575141，61307125，61420106006，61422509)

通信作者：*gjq@tju.edu.cn

低通滤波效应，不利于高频太赫兹波的探测。而传统的天线优化方法所带来的边际效应在逐渐减弱。一些优化天线性能的方法对设备和工艺的要求则越来越高，如高性能的 InGaAs 衬底需要低温分子束外延（MBE）生长且掺杂高浓度的过渡金属元素[61]，满足要求的设备在国际上极少，在国内仍处于空白。

出乎意料的是，2000 年开始的超材料研究却在多年之后推动光电导天线的研究进入了一个新的领域。超材料的研究起源于负折射率这一梦想的实现[62]，但超材料极高的设计自由度使其很快就超出了负折射率研究的范围，超材料成为一类最受关注的人工电磁媒质平台。超材料吸引了大批优秀的电磁学、光学、声学、热力学研究者投入其中，实现了诸如负折射率[62]、电磁异常增透[63]、电磁隐身[64-65]、连续域束缚态[66-67]、完美吸收[68-70]、超透镜[71-72]、等离激元诱导透明[73-75]、光学轨道角动量耦合[76-77]、光学拓扑绝缘体[78-80]和贝里相位控制[81-82]等一系列新颖奇异的功能。2007 年，超材料“跨界”到光电导天线的研究领域，而实现这第一步的是美国拉斯阿拉莫斯国家实验室的 O'Hara 等，他们在 2007 年的一篇会议文章中报道，将一个亚波长电学开口谐振环（eSRR）[83]与光电导发射天线的阳极电极相连，当泵浦光激励天线时，eSRR 结构内的电流被驱动，这些电流在 eSRR 中以特定的频率共振，从而增强了谐振频率附近的太赫兹波辐射[84]。自此超材料与光电导天线的交叉研究正式拉开了序幕。

用超材料优化光电导天线的方法是基于天线辐射、探测太赫兹波原理的。发射天线由半导体衬底及平行金属传输线组成，如图 1 所示，当有频率高于衬底禁带的飞秒光激励天线节时，该区域会形成大量的光生载流子，载流子在偏置电压作用下形成瞬态光电流，产生太赫兹脉冲辐射[29]。光电导天线辐射的太赫兹波有4种模式：正向辐射的远场辐射模式、背向辐射的远场辐射模式、传输线模式和衬底内传输的波导模式。而经典的太赫兹时域光谱系统只有效利用了远场辐射模式中背向传输的那部分能量，同时还会受硅透镜全内反射角的限制。探测天线的工作原理是基于发射天线的逆过程，即用背面入射的太赫兹波电场驱动天线中的光电流，而天线传输线则连接电流测量的系统，通过测量电流的大小和方向判断入射太赫兹脉冲在某一时刻的电场幅值和方向。

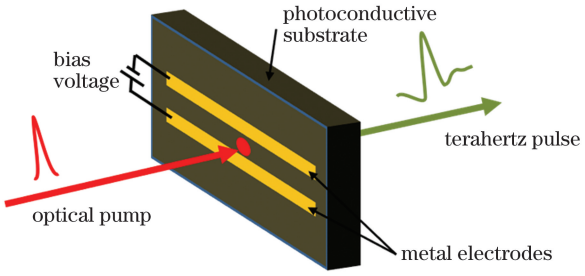

图 1 光电导发射天线的工作原理图

Fig. 1 Operation principle of photoconductive antenna emitter

用超材料改进光电导天线性能的方式有两大类，第一类与入射泵浦激光的局域化相关。超材料可以高自由度地操控透、反射泵浦光脉冲的振幅、相位和偏振特性[85]。目前，光电导天线技术中常用到的超材料可依据材料分为金属和介质两类。一般而言，金属上激发出的表面等离激元具有优异的电磁场局域能力，可以将光场紧紧束缚在微结构附近[86-90]，从而增强了衬底材料与入射光场的相互作用。但是到目前为止，基于金属人工结构的大部分超材料都受到高欧姆损耗的严重影响[91]，特别是在可见光和近红外波段。对于 50 nm 厚的光电导层，金属纳米结构的欧姆损耗最高可达 40%，严重劣化了引入结构所带来的益处[92]。近年来人们意识到介质超材料同样能形成场局域[93]且吸收损耗更低[94]，这类超材料一般由具有高折射率的介质柱微腔排列而成，这些亚波长微腔、光栅可以同时支持丰富的电场谐振模式和磁谐振模式，其对泵浦激光的调控能力更加强大[95]。

除用超材料控制泵浦激光与光电导衬底的相互作用外，直接调制光电导天线辐射/接收的太赫兹波是另一类超材料光电导天线的实现方式，通常这类超材料的尺度都在微米量级，O'Hara 等[84]研究的就是这类超材料。相比于泵浦激光，操控太赫兹波的方式更加灵活，因为正如上面所介绍的，光电导天线中有四种太赫兹波传播模式可供超材料大展身手，而且直接操控太赫兹波的另一个好处是易调整光电导天线的频谱特性。此外，光电导天线需要一个紧贴其后的超半球透镜匹配使用[58, 60]，其作用是准直（辐射天线）、聚焦（接收天线）太赫兹波，用介质超材料透镜替代超半球透镜可以让天线集成化程度更上一层楼。

为了进一步推动超材料光电导天线的研究，特别是推动国内相关研究的发展，本文梳理总结了超材料光电导天线研究的主要工作和重要进展，介绍了利用超材料提升光电导天线性能的方法，希望吸

引更多同仁投入到新型太赫兹辐射源和探测器的研究中，从而助力我国太赫兹技术的发展。文章的结构安排如下：第 2 节的内容是主要介绍纳米尺度超材料，其中 2.1 节介绍了集成纳米级金属超材料的光电导天线，而介质纳米超材料的内容则留在 2.2 节中；第 3 节总结了集成微米级金属超材料及操控光电导天线辐射的重要进展；第 4 节介绍了如何运用超材料替代超半球透镜以控制背向辐射的太赫兹波；最后第 5 节是总结与展望。

2 集成纳米超材料的光电导天线

2.1 金属纳米超材料

在光电导天线的光敏半导体衬底上引入金属纳米超材料可以有效提高光电导发射器的光-太赫兹波的转换效率以及光电导探测器的响应速度和灵敏度。其基本过程是：设计金属纳米超材料的几何结构，使入射泵浦光激发出的紧紧局域在超材料和半导体衬底界面处的表面等离激元谐振[63, 96]，而运用表面等离激元的方式则是八仙过海，各显神通。本节我们对具有代表性的若干工作进行了梳理，并介绍了其原理和效果。

在光电导天线中引入金属纳米超材料操控泵浦光的研究始于 2012 年，韩国 KAIST 的研究者将金属纳米光栅集成到 Bowtie 型光电导天线的天线节上，如图 2(a)所示。他们对这些纳米光栅的几何尺寸进行模拟计算，使得结构对中心波长为 800 nm、垂直偏振的泵浦光具有明显的表面等离激元谐振效应，这增强了 SI-GaAs 衬底对垂直偏振的泵浦光的耦合效率，从而提升了偏置电场最强处的载流子数目。如图 2(a)的频谱所示，金属纳米光栅有效提高了天线辐射的太赫兹波，在同样的偏置电压、入射功率和天线结构下，太赫兹辐射的功率最大增强了 3 倍[97]，而且光栅的引入没有引起天线频谱的改变，增强效果惠及整个工作频段。这种全频段的辐射功率增强首次向相关领域的研究人员展示了纳米超材料在操控飞秒泵浦激光上的巨大潜力和广阔前景，拓宽了在光电导天线上集成纳米超材料的研究思路，对后续研究工作具有重要意义。同年，该团队又设计了百纳米直径的银纳米岛，其替代纳米光栅结构被集成到光电导天线上，如图2(b)所示。该结构

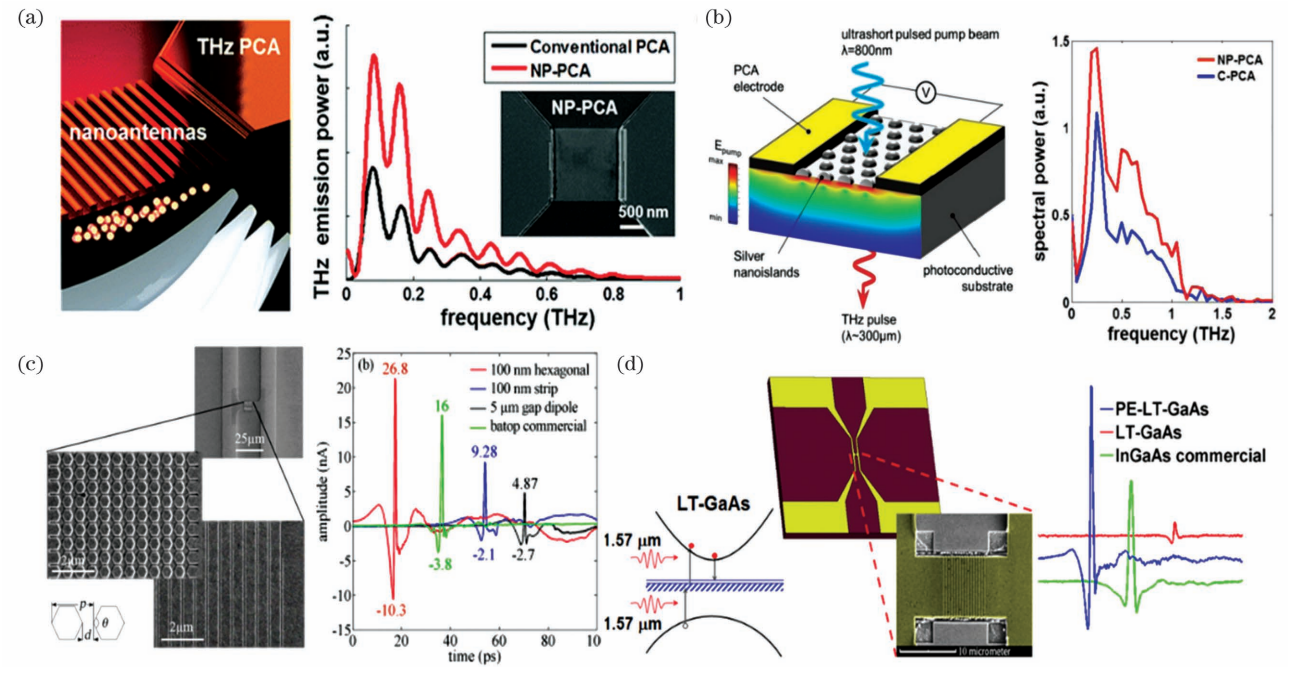

图 2 基于金属纳米超材料的光电导天线的相关工作。(a)集成金属纳米线栅的光电导天线示意图及其太赫兹频谱[97]；(b)集成银纳米岛的光电导天线示意图及其太赫兹频谱[98]；(c)集成六边形金属纳米结构阵列的光电导天线示意图及其太赫兹时域信号[99]；(d)集成金属纳米线栅的 1570 nm 光电导天线示意图及其太赫兹时域信号[102]

Fig. 2 Related works of PCA based on metal nano-metamaterials. (a) Schematic of PCA integrated with metal nano-gratings and its THz spectra[97]; (b) schematic of PCA integrated with Ag nano-islands and its THz spectra[98]; (c) schematic of PCA integrated with hexagonal metal nano-array and its THz time-domain signals[99]; (d) schematic of PCA integrated with metal nano-gratings pumped by 1570 nm femtosecond light and its THz time-domain signals[102]

增强太赫兹辐射功率的原理与金属纳米线栅相同，而优点在于易加工，利用镀膜工艺和金属薄膜的高温退火即可形成结构。实验结果表明，集成了纳米岛阵列的天线太赫兹辐射功率平均增强了两倍，同样地，在 0.1～1.1 THz 的工作频段上都观察到了太赫兹功率的增强，如图 2(b)中的曲线所示[98]。

类似原理的工作还有加拿大维多利亚大学研究者在 2014 年报道的集成在天线节上的六边形金属纳米结构阵列，如图 2(c)所示，他们将该结构调制的飞秒激光波长移到了 785 nm，同样用于最大化电流密度并增强太赫兹波辐射，尽管该结构上施加的偏置电压是商用太赫兹光导天线的 75%，但太赫兹发射场幅值增加了 60%，如图 2(c)中的曲线所示[99]。而该课题组更有意义的工作是从 2015 年陆续开展的用金属纳米结构操控衬底内载流子间接跃迁效率的研究[100-102]。早在 2000 年，伦斯勒理工大学的 Tani 等[34]指出，GaAs 衬底中的杂质和缺陷能级有助于载流子的间接跃迁，使光子能量明显小于 GaAs 禁带宽度的通信波段飞秒激光也能在 GaAs 衬底中产生载流子。但是后续研究都表明，这种载流子产生的外量子效率很低，在其他条件相同时，要获得相同的太赫兹电场幅值，所需的通信波段飞秒光的功率是 780 nm 飞秒光的 10 倍[103]。研究者设计了谐振波长位于 1570 nm 的金属纳米光栅，如图 2(d)所示，该波长的飞秒光在光栅上所形成的等离激元使得局域化的电场强度最大增强了 25 倍，使 1570 nm 飞秒光获得了与 800 nm 飞秒光同一量级的外量子效率，大大增加了衬底中的载流子数。如图 2(d)中的太赫兹时域信号所示，集成超材料的光电导天线辐射和探测的太赫兹脉冲幅值高于普通天线一个量级以上[102]。此外，利用金属纳米尺度的表面等离激元谐振增强或调控光电导天线上泵浦光与衬底相互作用的工作还有很多，结构五花八门，包括方块、圆柱体、纳米岛、六边形圆柱体、纳米沟槽等等，其原理相近，效果类似[104-115]，这里就不一一列举了。

金属纳米超材料除集成在天线节外，还可以直接作为天线的电极。相比于集成在天线节中，超材料构成的电极改变了天线的电学结构。由天线的工作原理可知，为了在光电导器件中高效地产生/探测太赫兹波，光生载流子迁移到天线金属电极上的传输时间应该在太赫兹振荡周期之内，但半导体衬底晶格内的载流子散射限制了载流子的输运速度，因此用超材料改变电极的结构可以将载流子输运长度限制在百纳米量级，这种方法不仅能增强发射/探测太赫兹波的效率，而且可以拓宽太赫兹脉冲的频谱。2012 年，研究者将间隔 100 nm 的交错排布的金属纳米光栅直接作为光电导探测天线的电极，如图 3(a)所示，通过表面等离激元效应将 830 nm 泵浦光更有效地耦合进空隙里，这些小空隙使得 GaAs 衬底里的光生载流子快速到达电极，实现了高效、宽带的太赫兹探测。优化后的天线探测到的太赫兹时域信号的峰峰值是商用光电导天线(BATOP PCA-800 nm)的 2 倍，比 20 μm 间隔的普通天线高约 40 倍，探测带宽与商用天线相当，比普通天线宽了 1 倍[116]。2013 年，密歇根大学的研究者将 Bowtie 型光电导天线(泵浦光激发波长为 800 nm)的电极用金属纳米光栅替代，如图 3(b)所示，发现光栅的表面等离激元起到了增强透射的作用，提高了量子效率，而且表面等离激元将载流子生成区域紧紧束缚在金属光栅下面很薄的一层衬底内，减少了光生载流子在天线衬底里的平均输运路径，提升了天线的响应速度。他们验证了这一方法既能增强发射天线的光-太赫兹波的转换效率，也能改善探测天线的响应率和探测灵敏度[117]。此后，该课题组进一步改进了光栅的设计，如图 3(c)所示，通过对 LT-GaAs 衬底进行刻蚀，形成了纵横比很高的梯形光栅结构，然后在其侧壁上镀一层金属形成三维电极。大多数光生载流子在距电极百纳米级范围内的衬底内产生，并在亚皮秒时间范围内漂移到天线上，有效地提高了太赫兹波的产生效率。图 3(c)中的实验结果表明，在 1.4 mW 泵浦光激励下，天线辐射的宽带太赫兹波(0.1～2.0 THz 内)的功率可达 105 μW，光-太赫兹波的转换效率达到 7.5%[118]。不过，这种三维光栅需要复杂的制备技术，因此加工比较困难。

等离子体纳米电极不仅可以增强天线节对泵浦光的吸收，还可以局域增强天线节上被施加的偏置电场。2015 年，研究者通过系统的实验研究，展示了基于三种不同类型纳米电极的 H 型偶极子天线(泵浦光波长为 790 nm)对偏置电场的操控能力，如图 3(d)所示。该工作指出，基于表面等离激元的太赫兹辐射功率增强作用是有限的，天线性能的进一步提升必须涉及偏置电场的操控；而且在小光功率密度的情况下，局域偏置场的影响比表面等离激元效应的影响更为显著[119]。类似的通过改进电极结构来改善光电导天线性能的研究还在开展

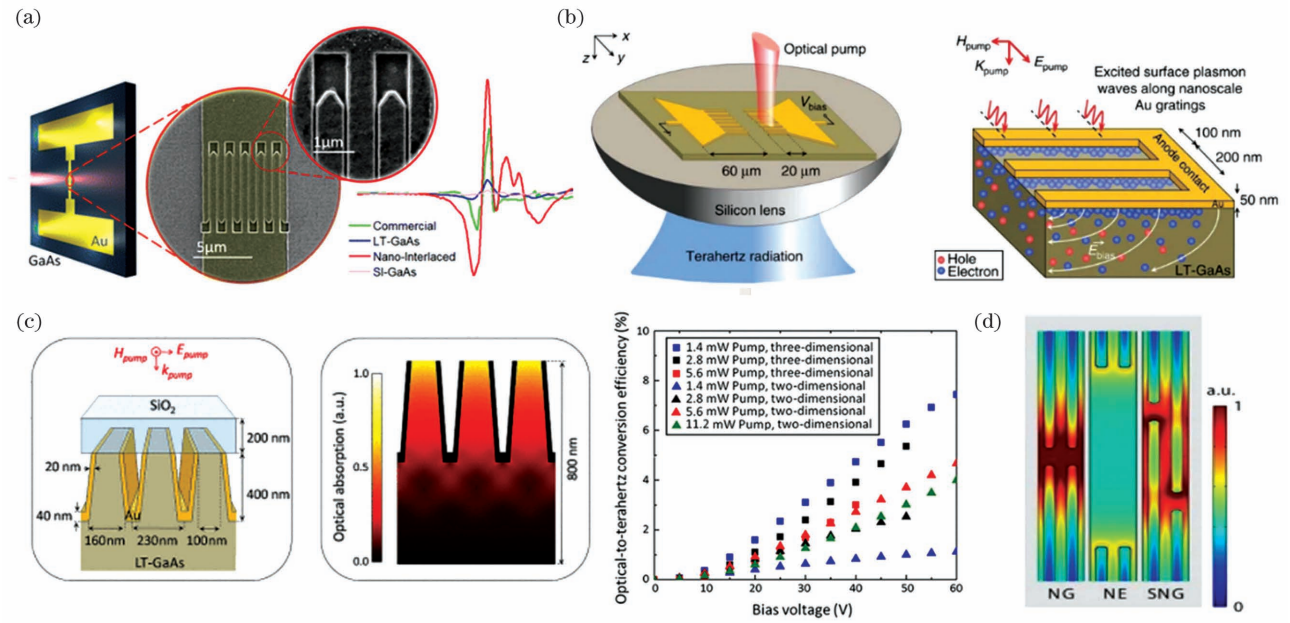

图 3 基于金属纳米电极的光电导天线的相关工作。(a)电极交错排布的光电导天线示意图及其太赫兹时域信号[116]；(b)电极为纳米光栅型的 bowtie 型光电导天线示意图及工作原理图[117]；(c)光电导天线的三维电极示意图和泵浦光场分布图以及天线的光-太赫兹波的转换效率曲线[118]；(d)H 型偶极子天线的纳米电极上的偏置场分布图[119]

Fig. 3 Related works of PCA based on metal nano-electrodes. (a) Schematic of PCA with interlaced structure and its THz time-domain signals[116]; (b) schematic and operation principle of bowtie PCA based on metal nano-electrodes[117]; (c) schematic and pump electric field distribution of 3D nano-electrodes of PCA, and optical-terahertz conversion efficiency of 3D PCA [118]; (d) bias field distribution on nano-electrodes of H-type dipole antenna[119]

中[120-125]，这些成果推动了金属纳米超材料在光电导天线上的应用。

以上介绍的研究工作都是基于单个天线结构，为了解决天线辐射功率不足这一核心问题，近年来，研究者们将超材料融入到天线阵列的优化研究之中。单个光电导天线受天线节有限面积和衬底热击穿的限制，所能承受的泵浦光功率和偏置电场强度都很有限。而呈阵列排布的多个光电导天线则可以有效增加激发区域的整体面积，是解决光电导天线功率微弱的最直接方法，可将太赫兹功率提高一个数量级以上，而有了超材料的加入，光电导天线阵列辐射的太赫兹功率还能更高、带宽还能更宽。2014 年，加州大学的研究者对以 GaAs 为衬底的大面积光电导天线阵列开展了系列化的研究[126-133]。如图 4(a)所示，该天线采用纳米光栅型电极，除了能提高天线的量子效率，还能增加天线节的有效面积，且可以减弱高泵浦光功率下的载流子屏蔽效应和衬底的热击穿。如图 4(a)中的实验结果所示，在泵浦光功率为 320 mW 的条件下，辐射的太赫兹脉冲功率高达 1.9 mW(频率范围为 0.1～2 THz)，光-太赫兹波的转换效率为 0.6%[126]。需要指出的是，这个工作需要利用微透镜阵列将泵浦光束分裂并聚焦到每个天线的天线节上，这无疑会增加系统的复杂度。随后他们在文献[127]中展示了一种不需要借助微透镜阵列聚焦泵浦光的大面积天线阵列，该天线的阳极同样采用金属纳米光栅型电极。为了避免全面积泵浦下相反偏置区域辐射的太赫兹波发生相消干涉，相邻天线之间的衬底被上层金属条遮挡而不能产生载流子，因此该天线同样能实现较大面积的光激发，从而避免较高光密度激发下的饱和效应，将天线性能提高到一个新高度，实验展示的光-太赫兹波的转换效率达到了 1.6%，频率更是拓宽到了 5 THz。他们在文献[128]中将大面积天线阵列与分布式布拉格反射层相结合，天线的光-太赫兹波的转换效率进一步增大到了 2.3%。类似地，他们将这种设计用于通信波长激励的光电导太赫兹发射器中，实验获得了高达 300 μW 的太赫兹辐射，带宽超过了 5 THz[129]。

大面积等离激元天线阵列不仅具有上述工作中介绍的增强太赫兹辐射的能力，还能实现太赫兹波的高灵敏度探测[130-133]。图 4(b)展示了此类超材料天线阵列的光学透射/吸收特性，结果表明，这种大面积的结构使得衬底在泵浦光中心波长附近具有高吸收率，在纳米尺度上促进了入射太赫兹波和泵浦

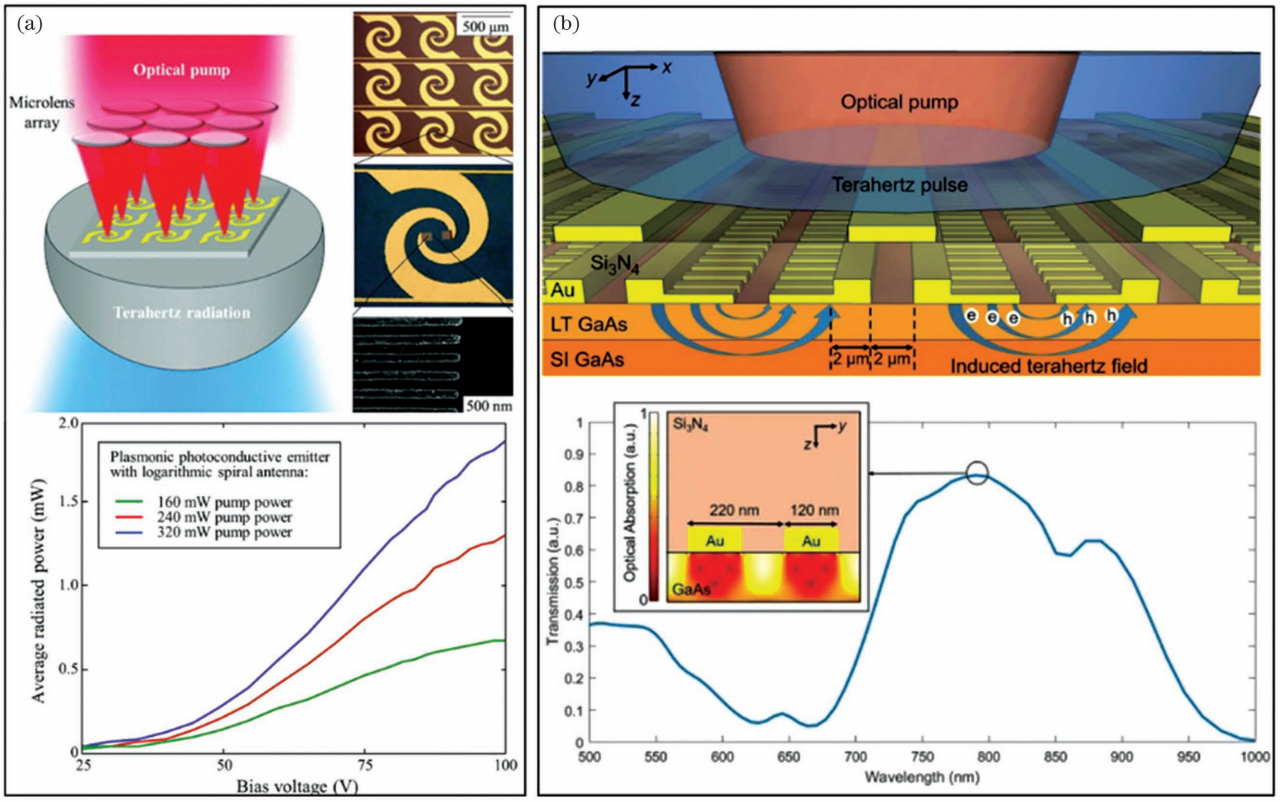

图 4 基于金属纳米超材料的光电导天线阵列的相关工作。(a)等离子体光电导发射天线阵列的示意图及其辐射功率谱[126];(b)大面积等离子体光电导探测天线阵列的示意图及其光学透射/吸收特性[130]

Fig. 4 Related works of PCA array based on metal nano-metamaterials. (a) Schematic and average radiated power spectra of plasmonic PCA emitter array[126]; (b) schematic of large-area plasmonic PCA detector array and its optical transmission/absorption characteristics [130]

光之间的相互作用[130]。2021 年,伊朗伊斯兰自由大学的 Balow 等[134]也研究了类似的大面积表面等离激元探测天线阵列,不同的是他们采用了纳米阶梯式电极,数值计算结果表明,该天线在 50 mW 泵浦光激励下可将超过 95%的泵浦功率传输到 GaAs 衬底上,产生了 215 nA 的光电流(与采用矩形电极的天线相比,该值提高了 25%),探测带宽可达到 0.1~8 THz。

对以上介绍的金属纳米超材料光电导天线的性能参数进行了总结,如表 1 所示,其中 SNG 和 NE 是图 3(d)所示的两种具有纳米电极的 H 型偶极子天线。虽然本文重点关注的是辐射和探测太赫兹脉冲的光电导天线,但相近的光敏过程意味着金属纳米超材料在光混频天线上也可以大有作为,而光混频天线在通信和成像等领域也有重要的应用价值。2013 年,新加坡科技研究局的 Tanoto 等[135]将尖端相对(tip-to-tip)型纳米间隙电极结构(阳极与阴极间最小距离为 100 nm)集成到光混频天线的两个电极上,如图 5(a)所示。用于混频的激光器的中心波长分别是 852 nm 和 855 nm,tip-to-tip 型电极结构可以局域泵浦光和太赫兹波的电场。与交叉电极天线相比,tip-to-tip 型天线的辐射强度增强了约 2 个数量级,辐射带宽覆盖到 1.3 THz,如图 5(a)中的频谱所示 。Berry 等[136-139]将原来用在光电导天线上的金属纳米光栅移到了光混频天线上。他们将图 5(b)中所示的纳米光栅型电极应用于 1550 nm ErAs: InGaAs 衬底的光混频天线上,同样地,他们利用表面等离激元电极的独特性能缩短了光载流子到电极的平均传输路径,增加了驱动太赫兹天线的超快光电流,从而显著提高了效率。由图 5(b)中的太赫兹辐射功率曲线可知,在 150 mW 泵浦功率下,该天线在每个连续波辐射周期内最高可辐射 0.8 mW 的太赫兹波(1 THz 处)[137]。他们在文献[139]中还进一步分析了集成超材料的 780 nm LT-GaAs 衬底光混频天线的频谱特征以及太赫兹频谱与泵浦光频谱特征之间的依赖性。

表 1 基于金属纳米超材料的光电导天线的性能对比

Table 1 Performance comparison of PCA based on metal nano-metamaterials

Ref.	Pump wavelength /nm	Pump power /mW	Bandwidth / THz	Peak-to-peak enhancement factor	THz power / mW	THz power enhancement factor
[97]	800	60	0.10-1.10	-	-	2.4
[98]	800	150	0.10-1.10	-	-	2
[99]	785	10	0.10-2.00	-	-	2.56
[102]	1570	25	0.10-2.43	-	-	10^2
[116]	830	-	0.10-1.80	41	-	-
[117]	800	5	0.10-1.50	-	-	50
[118]	800	1.4	0.10-2.00	-	0.105	-
[119]	790	350	0.10-3.00	-	0.17(SNG)/0.24(NE)	23(SNG)/32.9(NE)
[126]	800	320	0.10-2.00	-	1.9	-

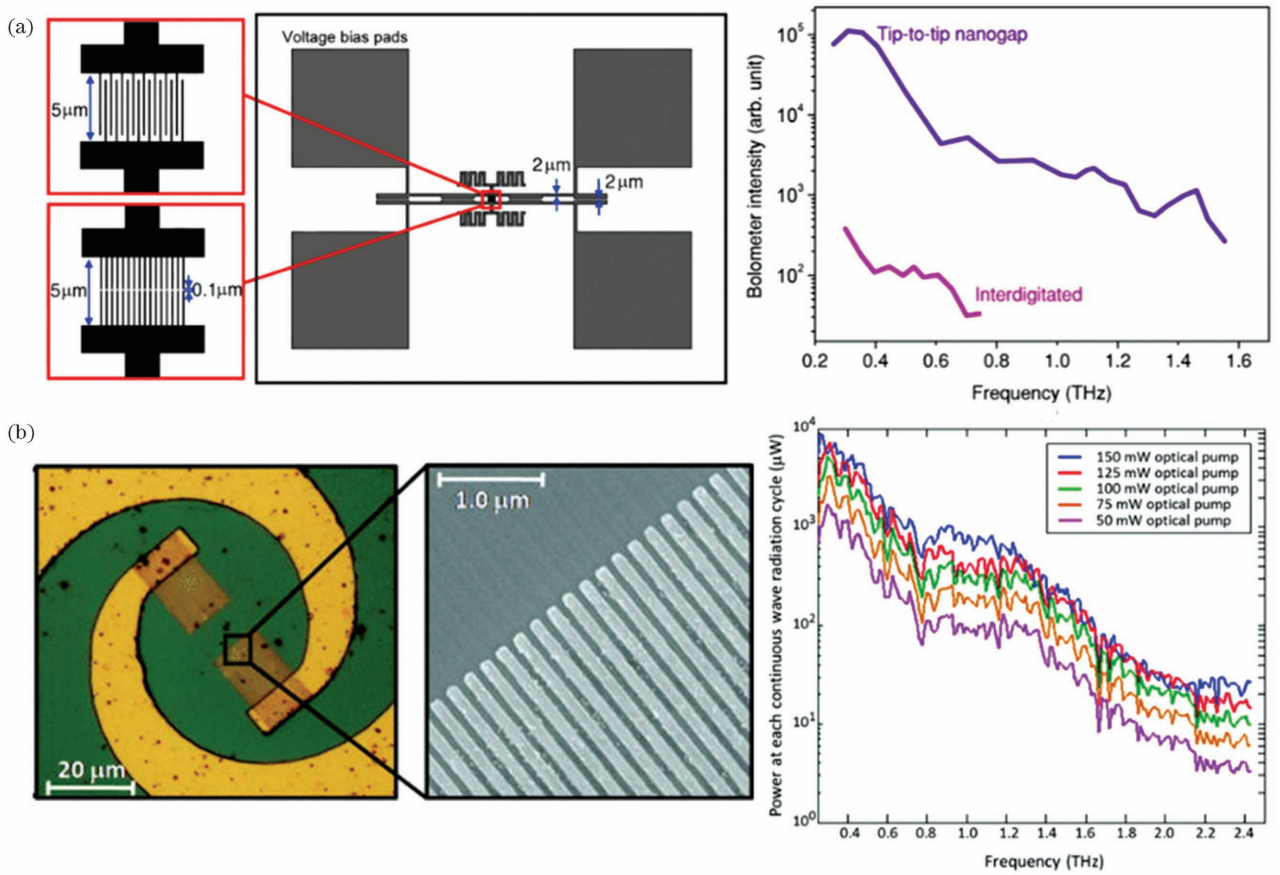

图 5 基于金属纳米超材料的光混频天线的相关工作。(a)电极呈交错排布的 tip-to-tip 型光混频天线示意图及其输出强度对比[135];(b)等离子体光混频天线示意图及太赫兹辐射功率[137]

Fig. 5 Related works of photomixers based on metal nano-metamaterials. (a) Schematic and output intensity of CW THz photomixer with interdigitated electrodes and tip-to-tip nano-gap electrodes[135]; (b) schematic and radiated THz power of plasmonic photomixer[137]

2.2 集成介质纳米超材料的光电导天线

全介质超材料由于不存在欧姆损耗和耐热性的问题,近年来受到越来越多的关注。2017 年,伊朗扎伊尔德大学的 Khorshidi 等[140]从理论上提出了一种可以传输更多泵浦光到光电导天线衬底上的周期性介质条结构,仿真结果表明,该结构能够将横向偏振泵浦光(波长为 0.7~1.0 μm)功率的 90%传输到衬底上。通过对天线模型的分析,引入介质条降低了泵浦光的反射率,衬底中的光生载流子数量增加,从而光-太赫兹波的转换效率增大。第一个实

验验证全介质纳米超材料增强光电导天线探测效率的工作是伦敦大学学院的 Mitrofanov 等[141]在 2018 年报道的。如图 6(a)所示，他们设计的结构包括低温生长的 GaAs 纳米光栅阵列和亚表面分布式布拉格反射器。纳米尺度的介质结构可以捕获特定波段的泵浦光，从而增强光吸收，如图 6(a)中的吸收率曲线所示。在 0.5 mW 光激发下，该结构的引入使得太赫兹电场诱导的光电流与普通探测天线相比增加了一个数量级以上，信噪比达到了 10^6，实现了灵敏、高效的太赫兹波探测。此后 2019 年，该课题组研究了集成纳米 GaAs 微腔的探测天线，如图 6(b)所示，在未集成布拉格反射器的情况下，利用微腔的电、磁偶极子谐振实现了对泵浦光(偏振沿微腔连接方向)的完美吸收，如图 6(b)中的归一化曲线所示。集成这种超材料的光电导太赫兹探测器可在较低泵浦功率下实现快速响应，利用 100 μW 的超快激光激发，实现了比 GaAs 薄膜高 6 个数量级的太赫兹探测信噪比[142]。

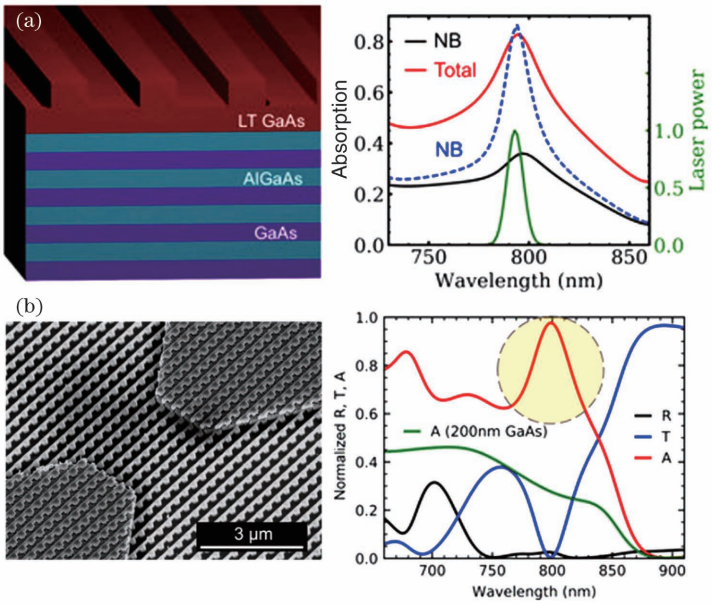

图 6 基于介质纳米超材料的光电导探测天线的相关工作。(a)全介质超材料增强光电导探测天线的示意图及其光学吸收谱[141]；(b)集成 GaAs 谐振器的光电导探测天线的扫描电镜图和模拟的超表面结构的吸收率、反射率和透射率以及 200 nm 平面 GaAs 衬底的吸收率，入射光为 800 nm，偏振方向沿 GaAs 谐振器连接方向[142]

Fig. 6 Related works of PCA detectors based on dielectric nano-metamaterials. (a) Schematic and optical absorption spectra of all-dielectric metamaterial enhanced PCA detectors[141]; (b) SEM photo of PCA detectors with GaAs resonators, simulated absorption, reflectivity, transmission of metasurfaces and absorption of 200 nm flat GaAs substrate for 800 nm incident light with polarization direction along GaAs resonator connection[142]

全介质超材料还可以与光电导发射天线结合以增大光-太赫兹波的转换效率。2020 年，天津大学的研究者通过直接在光电导天线衬底上刻蚀介质光栅阵列，实现了太赫兹辐射功率的显著增大，结构示意图如图 7(a)所示。引入纳米光栅的主要目的是为了抑制衬底对飞秒激光中心波长(780 nm)附近的反射，图 7(b)的实验结果展示了在偏振垂直于光栅的飞秒光泵浦下，纳米光栅结构的反射率降至 GaAs-空气表面的 2.53%，从而有效增加了 GaAs 衬底中产生的光生载流子。该工作利用图 7(c)所示的 4F 太赫兹时域光谱系统对发射天线的性能进行了测试，使用宝石硅(Silicon-on-sapphire，SOS)光电导探测天线进行太赫兹波的探测。为了保证测量的精确性，4F 系统进行了针对性的改进：首先是增加反射显微成像系统来监测天线上的纳米结构与泵浦光的相对位置；第二点是为硅透镜单独安装了一个三维平移台，并利用一个 3D 打印的支架将硅透镜压在天线衬底后表面，因此硅透镜与入射泵浦光位置可保持相对不变。在偏振垂直于光栅的泵浦光的激励下，天线辐射太赫兹波的时域与频域信号分别如图 7(d)和 7(e)所示，与传统光电导天线相比，超材料发射天线在 0.05～1.6 THz 范围内实现了 3.92 倍的太赫兹功率增强。值得一提的是，该工作还数值研究了纳米光栅对偏置电场的影响，如图 7(f)所示，全介质纳米光栅的引入不仅能最大限度地增加了衬底表面产生的光生载流子，而且还有

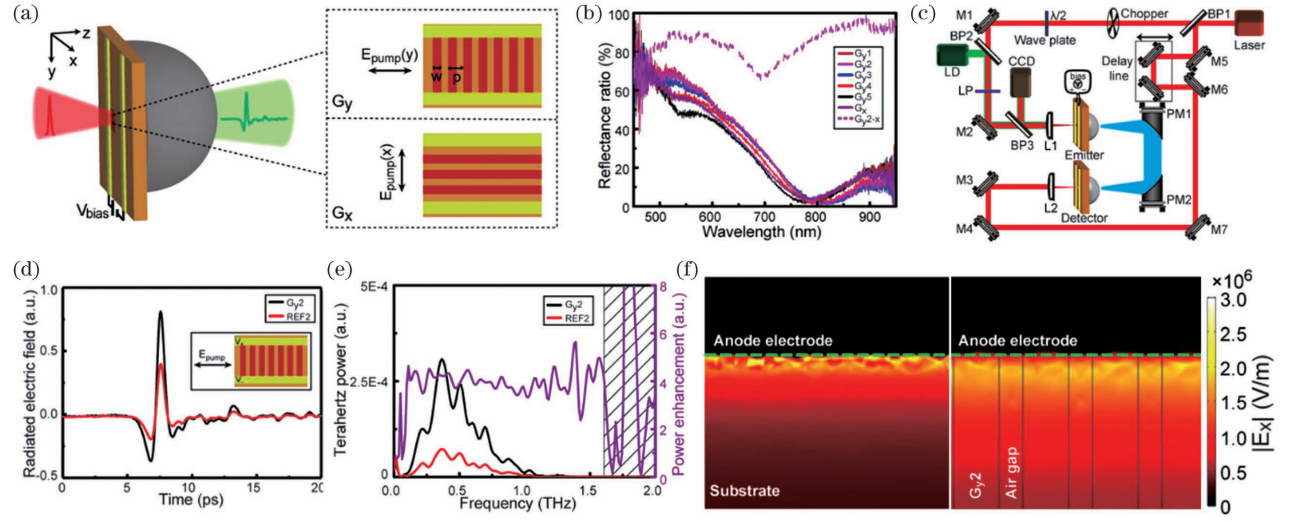

图 7 基于介质纳米超材料的光电导发射天线[143]。(a)超材料光电导发射天线及纳米光栅结构示意图;(b)纳米光栅的光学抗反射效应;(c)4F 太赫兹时域光谱系统及反射显微成像系统原理图;(d)超材料光电导发射天线和传统发射天线的太赫兹波时域信号;(e)超材料光电导发射天线和传统发射天线的太赫兹功率谱及其增强因子;(f)仿真的平面 GaAs(左图)与光栅结构(右图)上施加的偏置电场

Fig. 7 PCA emitters based on dielectric nano-metamaterials[143]. (a) Schematic of metamaterials-assisted PCA and unit cells; (b) measured optical anti-reflectance effect of nanograting; (c) schematics of 4F THz time-domain spectroscopy system and added reflective microscopic imaging system; (d) THz time-domain signals of metamaterials-assisted PCA emitter and traditional PCA emitter; (e) THz power spectra of metamaterials-assisted PCA emitter and traditional PCA emitter as well as power enhancement; (f) simulated bias electric field distributions of flat GaAs (left) and nanograting (right)

利于增强施加在光生载流子上的偏置电场[143]。这一研究将纳米结构对泵浦光和偏置电场的影响同时考虑进去,为后面的研究提供了新的思路。

最后,为了帮助读者更好地了解这些工作,我们对以上介绍的介质纳米超材料光电导天线的性能参数进行了总结,如表 2 所示。

表 2 基于介质纳米超材料的光电导天线的性能对比

Table 2 Performance comparison of PCA based on dielectric nano-metamaterials

Ref.	Pump wavelength / nm	Pump power / mW	Bandwidth / THz	Signal-to-noise radio	THz power enhancement factor
[141]	800	0.5	0.10–4.00	10^6	–
[142]	800	0.1	0.10–1.10	10^6	–
[143]	800	10.0	0.05–1.60	–	3.92

3 集成微米超材料的光电导天线

本节介绍在天线上集成微米超材料的研究进展。正如第一节所述,超材料光电导天线的研究正是从 2007 年 Hara 将 eSRR 作为天线电极开始的。当泵浦光激励天线时,eSRR 结构内的电流被驱动,这些电流在 eSRR 中以特定的频率共振,从而增强了谐振频率附近的太赫兹波辐射。泵浦光激发位置不同,辐射的太赫兹波的峰值电场和频谱特征有较大差异,利用这种 eSRR,天线辐射的低频太赫兹波被增强三倍之多[84]。2011 年,日本大阪大学的 Takano 等[144]在光电导发射天线金属电极旁集成了典型的金属开口谐振环(SRR),如图 8(a)所示,太赫兹辐射会受到 SRR 的影响,因此该结构实现了太赫兹辐射频谱和偏振的光开关。图 8(b)是集成图 8(a)中三种 SRR 结构的天线节受激发时天线辐射太赫兹波的振幅曲线。当有光脉冲入射到 SRR 上时,光生载流子引起衬底电容和电导率的变化,因此 SRR 的谐振频率和幅度都发生改变,这对太赫兹辐射的影响与 SRR 没被激发时大有不同[图 8(c)],从而实现了红外光对天线辐射特性的调控[144]。同年,美国犹他大学的 Liu 等[145]将波纹状金属光栅围绕在光电导探测天线的金属电极(偶极子)外侧,从而实现对多频段太赫兹波的相干探测增

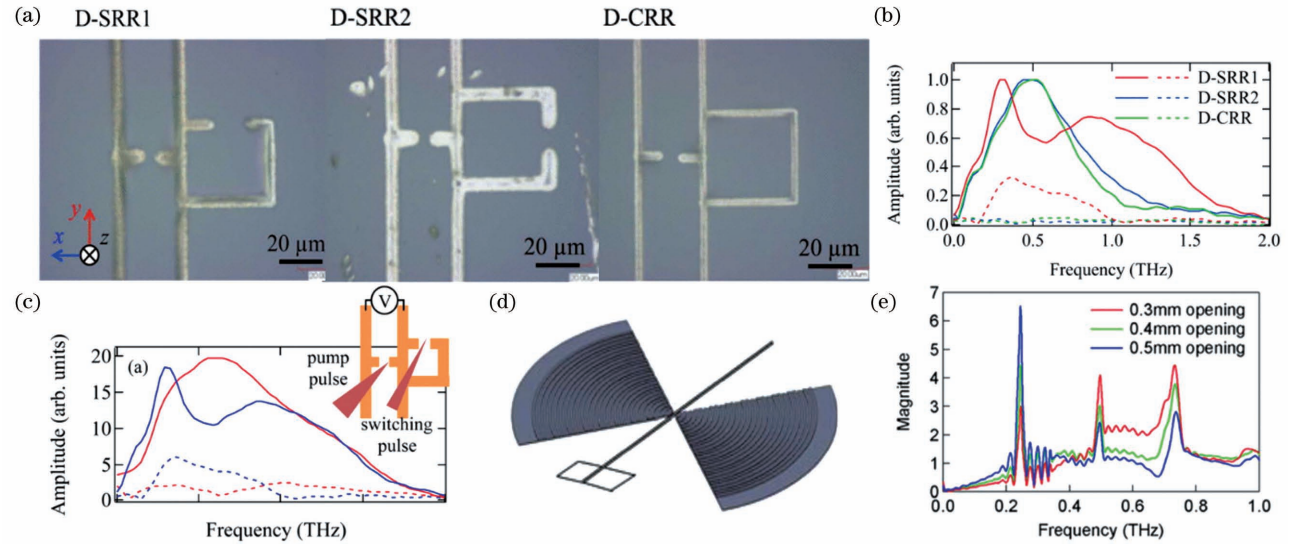

图 8 集成金属微米结构的光电导天线的相关工作。(a)旁连 SRR 微结构的光电导发射天线的显微镜图[144];(b)实验测得的天线辐射太赫兹波的振幅谱[144];(c)同时有泵浦光和开关脉冲激励的太赫兹波振幅谱与仅泵浦光激励下的太赫兹波振幅谱,实线和虚线分别是电场 x 偏振和 y 偏振下的测量结果,插图显示了泵浦光和开关脉冲的原理图[144];(d)集成波纹金属结构的光电导探测天线示意图[145];(e)相对于普通偶极子天线的灵敏度增强的归一化幅度谱[145]

Fig. 8 Related works of PCA integrated with metal micro-structures. (a) Micrographs of PCA transmitter with micron-SRR[144]; (b) measured THz amplitude spectrum radiated by emitter[144]; (c) measured amplitude spectrum of THz wave under both pumping and switching excitation and that under only pumping excitation with schematic of pump light and switch pulse shown in illustration and solid and dashed lines indicating measured results under electric field with polarization of x and y, respectively[144]; (d) schematic of PCA detector with corrugated metal structure[145]; (e) normalized amplitude spectra showing sensitivity enhancement relative to simple dipole antenna[145]

强,如图 8(d)所示,超材料结构的表面等离激元效应将入射的太赫兹脉冲耦合到结构表面并传输到探测天线上,在该过程中并未使用任何透镜对太赫兹波进行聚焦。如图 8(e)所示,利用结构的表面等离子激元共振,可提高探测天线对多个太赫兹频段的相干探测灵敏度。

在获得这些令人激动的进展之后,超材料光电导天线的研究却更多地集中在纳米结构上,而微米超材料的研究则趋于平静。直到近两年,这种方法又吸引了越来越多的人。2021 年,天津大学的研究者开始将超材料用于调控沿着共面传输线传播的太赫兹模式。正如第一节介绍的,这部分模式在传统的光电导天线中被浪费掉。天线结构示意图如图 9(a)所示,该工作通过在共面传输线上对称性地集成金属 SRRs 来操控这部分波。如果单从传输线的角度来看,SRR 是一个支路滤波器,数值模拟的结果也很好地验证了这一观点,相比于普通天线,新天线两侧的 SRR 间形成了谐振腔,谐振腔的谐振频率可以通过改变 SRR 尺寸参数来调节,如图 9(b)所示。但深入研究发现,SRR 还能对远场辐射产生影响,这是支路滤波器理论不能解释的。这种 SRR 不仅能对太赫兹远场辐射频谱进行滤波,重要的是,SRR 的引入从总能量上实现了辐射功率的增强。通过不同样品的多次测量和取平均,这种滤波和增强得到了统计结果的支持,如图 9(c)所示。运用时域数值模拟发现,与参考天线相比,SRR 不仅会反射沿传输线传播的模式,而且能将之散射到自由空间中形成新的太赫兹背向辐射源,如图 9(d)所示,这部分被重新散射到远场的太赫兹波使天线的总功率高于传统天线。而 SRR 散射源间的干涉相长相消频率则受 SRR 与天线节的间距调控,不同远近的 SRR,其太赫兹频谱中的干涉峰、谷个数不同,频率也发生变化,如图 9(e)所示。而当 SRR 分别分布在传输线内侧和外侧时,其带通和带阻对应的频率对调,如图 9(f)所示,其他 SRR 的几何参数也对频谱有着或多或少的影响。这种通过在传输线上集成 SRR 操控太赫兹波散射的方法不增加光电导天线的加工难度,却能将总功率提升 1.55 倍,并能灵活操控辐射太赫兹波的频谱特征,为超材料光电导天线的研发提供了新的研究思路[146]。除在传输线上集成微结构外,另一种增强太赫兹辐射的方法是通过在光电导天线衬底的背面设计微结构来增强从衬

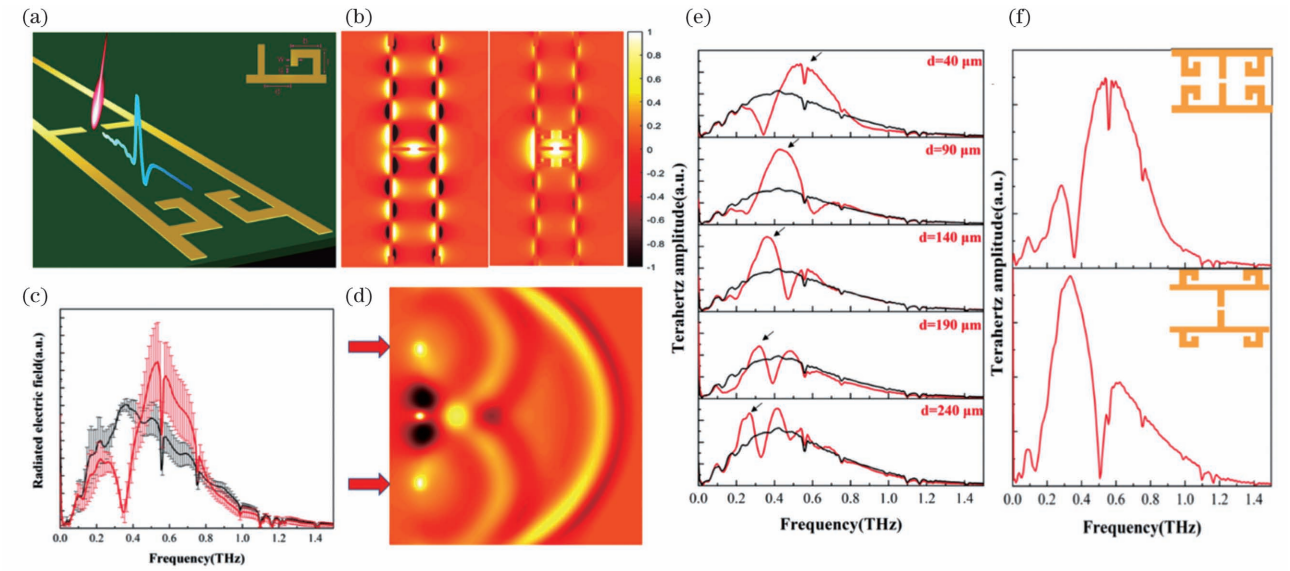

图 9 集成金属微米 SRR 的光电导天线[146]。(a)集成 SRR 的超天线的结构示意图;(b)数值仿真的参考天线(左图)和超天线(右图)在 0.54 THz 处的传输线模式的太赫兹场分布;(c)带有均方根误差条的平均太赫兹振幅谱;(d)超天线的太赫兹波辐射过程;(e)随 SRRs 与天线节的间距 d 变化的超天线的太赫兹振幅谱;(f)SRRs 分别在传输线内/外侧时的太赫兹频域振幅谱

Fig. 9 PCA integrated metal micro-SRR[146]. (a) Schematic of meta-antenna with SRRs; (b) simulated electrical field distributions along coplanar lines of reference PCA (left) and meta-antenna (right) at 0.54 THz; (c) averaged THz amplitude spectra with root mean square error bars; (d) THz radiation process of meta-antenna; (e) THz amplitude spectra of meta-antennas with various distances d between SRRs and gap; (f) measured amplitude spectra of meta-antenna with SRRs inside/outside coplanar lines, respectively

底出射到空气中的太赫兹波。2020 年,上海师范大学的 Zhao 等[147]提出了一种 T 形谐振器,通过将结构集成至光电导天线衬底背面,实现了太赫兹超材料的准近场激发,该设计仍需要超半球硅透镜来保证太赫兹波传输到自由空间的高耦合效率。T 形谐振器在谐振频率上具有更高的 Q 值,天线辐射的太赫兹波在耦合到自由空间之前会在近场内激发该结构,从而导致辐射的太赫兹频谱在 0.47 THz 附近有一个宽带的增强,在 0.92 THz 附近有一个极窄的增强。

4 集成超材料操控辐射的太赫兹波

前面对超材料影响太赫兹脉冲的辐射过程进行了梳理和介绍,本节介绍通过集成超材料,对辐射的太赫兹脉冲进行操控的相关研究进展。该方面的一个发力点是构建全介质超透镜,替代超半球硅透镜准直光电导天线辐射的太赫兹波。

传统的太赫兹透镜是通过传播路径上空间相位的累积来实现对入射波的聚焦,因此不同的相位分布要靠材料的厚度变化来调节,这不利于集成化和小型化。而基于超表面的太赫兹透镜,即太赫兹超透镜,是通过在界面上用人工微结构引入一定的相位梯度,进而改变出射波前的形状。最早的太赫兹超透镜大多采用单层金属结构,例如 V 形天线[148-149]、C 形开口谐振环[150]和矩形天线[151]等。2015 年,天津大学的 Wang 等[150]提出了一种基于共振相位的 C 形铝制微结构的平面超透镜,通过调节其几何形状和开口大小,并通过旋转 180°,实现了 2π 的相位覆盖范围,并保证透过率均有较高的水平。该透镜直径为 5.52 mm,焦距为 10 mm,数值孔径为 0.27,并在 0.5~0.9 THz 的范围内都表现出良好的聚焦特性。基于共振相位和几何相位原理的单层超透镜,由于偏振转换带来的影响,透射效率固有的上限为 25%。金属-介质-金属的“三明治”结构[152-154]可以增大透射效率,但是由金属谐振器组成的超透镜存在欧姆损耗,而基于全介质的超表面可以打破这一固有限制,且通过合理的设计,介质谐振器可以同时支持电偶极响应和磁偶极响应,并实现 2π 的相位覆盖范围。近年来,许多研究工作都表明,全介质为设计高效平面太赫兹聚焦透镜提供了理想的平台[155-157]。例如,2018 年,重庆大学的研究者提出了一种全介质超透镜并从理论和实验上进行

了验证，其单元结构为沉积在 SiO_2 表面上的 Si 柱，尺寸为 0.39λ（工作波长 λ 为 118.8 μm），透镜的焦距和半径均为 300λ，数值孔径为 0.707，聚焦时最大入射角度可达 48°[157]。值得一提的是，超透镜上每个单元结构强烈的模式色散会使得超透镜存在较大的色差，从而导致不同频率的太赫兹波无法会聚到同一焦点上，这会严重阻碍其宽带应用。目前，可见光和红外波段的超透镜宽带消色差研究已取得了长足的发展，但在太赫兹波段，由于基础材料的选取、单元结构的设计以及样品加工等方面与其他波段有着显著的差别，消色差超透镜目前只有很少的研究[158-159]。

如上所述，关于太赫兹超透镜研究的工作不胜枚举。基于太赫兹超透镜的集成化和小型化将太赫兹超透镜与光电导天线相结合，有助于进一步提高太赫兹时域光谱系统的集成化程度。超透镜不仅比超半球硅透镜体积小，且有望将抛物面镜的功能也合并进来，发展超透镜是新颖且有前景的简化太赫兹系统光路的方法。2017 年，天津大学的研究者提出并数值上展示了一种硅基超表面透镜，专门用来准直光电导天线辐射的太赫兹波，如图 10(a)所示。与超半球硅透镜不同，超表面透镜更薄更轻且紧贴在天线背面。其功能是将特定波长的太赫兹辐射直接准直为平面波出射，达到将超半球硅透镜和后面抛物面镜的功能合二为一的目的。超表面透镜由 200 μm 厚的高阻硅亚波长方柱排列构成，用不同的方柱边长来调控太赫兹波的传输相位。数值模拟结果如图 10(b)展示，远场辐射的模式图中虽然存在旁瓣，但大部分能量都紧密地围绕光轴。而如图 10(c)所示，在频率 1 THz 处，天线节辐射的太赫兹波在经过超表面透镜后发散角被大幅度压缩，透镜输出的光束是近乎平行的光束，即天线辐射的类球面波被超透镜准直成准平面波并传播到 20 mm 后才显著发散[155]，模拟结果完全验证了这种超透镜的设计，有望在未来实现直接集成到光电导发射天线背面的超表面透镜。

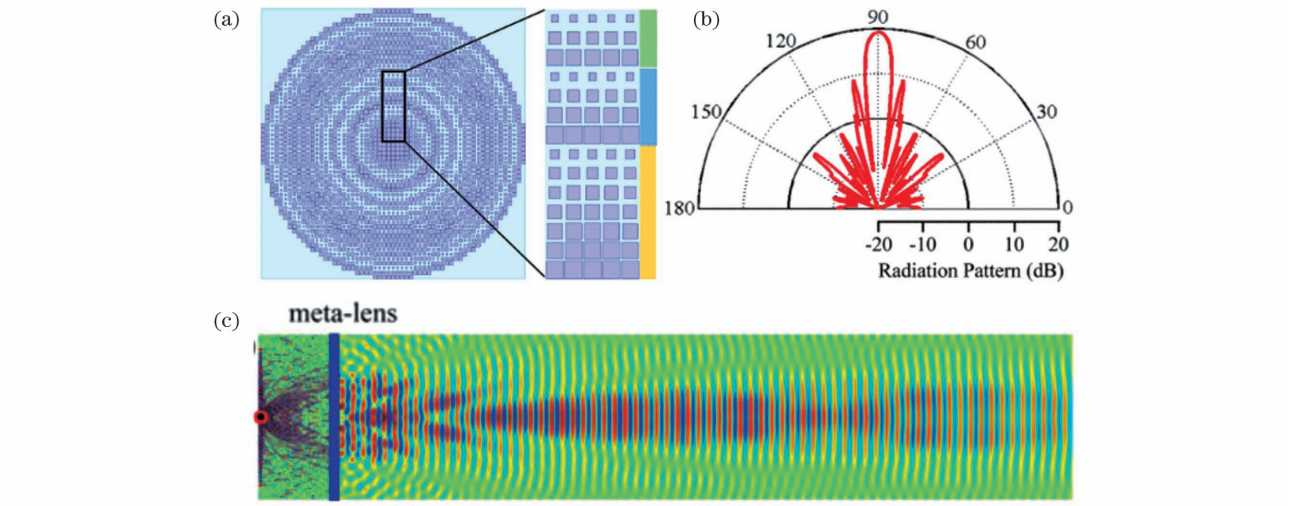

图 10 集成介质超透镜的光电导天线[155]。(a)设计的用于光电导天线的全介质超透镜的前视图；(b)超透镜的远场辐射模式；(c)模拟的通过超透镜传输的太赫兹波(频率为 1 THz)的电场分布图

Fig. 10 PCA integrated with dielectric meta-lens[155]. (a) Front view of all-dielectric meta-lens designed for photoconductive antenna; (b) far-field radiation mode of meta-lens; (c) simulated electric field profile of THz wave (1 THz) propagating through meta-lens

与第二节和第三节的内容相比较可发现，现有的用超材料辅助光电导天线的工作大多是调控太赫兹波的功率及频谱，关于太赫兹波波束整形的研究相对缺乏，因此充分利用超材料的特性对太赫兹波的波前进行控制是后续发展的方向之一，也是颇具价值的一个研究方向。而如何利用纳米超材料构建相位梯度超表面使得光电导天线产生具有特定角度的太赫兹波是一个难点，尚待解决。

5 结束语

首先简要而系统地介绍了一系列集成纳米级金属/介质超材料的光电导天线的相关工作，这些工作是从纳米超材料对飞秒激光和载流子输运机制的影响这一角度出发，利用纳米结构局域增强衬底对泵浦光的吸收能量，大幅度提高光电导发射器的光-太赫兹波的转换效率和光电导探测器的响应速度、灵

敏度；通过改变光电导天线的电极形状，可以减少载流子跃迁到电极上的时间，进而改善太赫兹光电导天线的性能；此外，通过构建集成纳米电极的天线阵列和增加泵浦光激发区域面积，可以提高衬底可承受的泵浦功率的上限，从而避免较高光功率密度激发时产生的饱和效应。还介绍了基于微米级金属/介质超材料的光电导天线，通过在天线电极上或衬底背面设计微米结构，可以有效调控太赫兹辐射的频谱特征和传播特征。

纵观超材料光电导天线的发展，其还处于研究初期，相信在未来有更多功能新颖的超材料会被引入到光电导天线的优化中来，同时一些新材料的加入可能会引起研究方式的根本变化，一个较近的突破点是石墨烯、黑磷等二维材料的运用[160-162]。例如 Fakhar 等[160]在 2020 年提出了一种新方法并利用 COMSOL 软件进行了仿真研究，利用 800 nm 泵浦光激发光电导天线辐射太赫兹波，太赫兹波被耦合到与天线相结合的石墨烯表面波波导中，形成太赫兹表面波。但是，该工作对石墨烯的电子迁移率要求较高(10^5 $cm^2 \cdot V^{-1} \cdot s^{-1}$)，在样品实际加工过程中石墨烯的电子迁移率较难达到 10^5 $cm^2 \cdot V^{-1} \cdot s^{-1}$，因此该方法在推广上还面临困难。另一个发力的方向，是将超表面调控波前的能力运用到光电导天线的优化中，一种可能的方法是基于超材料对电磁波波前控制的原理[163-165]，构建具有相位梯度的超材料与光电导天线相结合，对太赫兹波进行高自由度的波前调控。最后还要强调的是，基于光混频天线在太赫兹通信领域的重要地位，利用新型超材料实现光混频天线的主动调控，其价值和意义越发重要，也是超材料光电导天线未来的发力点之一。总之，这些新颖的天线结构在太赫兹领域具有巨大的应用潜力，有望从根本上推动光电导天线的发展，显著增强当代太赫兹光电导器件的性能。

参 考 文 献

[1] Stoik C D, Bohn M J, Blackshire J L. Nondestructive evaluation of aircraft composites using reflective terahertz time domain spectroscopy [J]. Optics Express, 2008, 16(21): 17039-17051.

[2] Yakovlev E V, Zaytsev K I, Dolganova I N, et al. Non-destructive evaluation of polymer composite materials at the manufacturing stage using terahertz pulsed spectroscopy [J]. IEEE Transactions on Terahertz Science and Technology, 2015, 5(5): 810-816.

[3] Ulbricht R, Hendry E, Shan J, et al. Carrier dynamics in semiconductors studied with time-resolved terahertz spectroscopy [J]. Reviews of Modern Physics, 2011, 83(2): 543-586.

[4] Kawase K, Ogawa Y, Watanabe Y, et al. Non-destructive terahertz imaging of illicit drugs using spectral fingerprints[J]. Optics Express, 2003, 11(20): 2549-2554.

[5] Ahi K, Shahbazmohamadi S, Asadizanjani N. Quality control and authentication of packaged integrated circuits using enhanced-spatial-resolution terahertz time-domain spectroscopy and imaging[J]. Optics and Lasers in Engineering, 2018, 104: 274-284.

[6] Minin I V, Minin O V. THz quasioptics applications in security [J]. Proceedings of SPIE, 2006, 6212: 621210.

[7] Federici J, Moeller L. Review of terahertz and subterahertz wireless communications[J]. Journal of Applied Physics, 2010, 107(11): 111101.

[8] Saeedkia D. Handbook of terahertz technology for imaging, sensing and communications [M]. Cambridge: Woodhead Publishing Limited, 2013.

[9] Yang X, Zhao X, Yang K, et al. Biomedical applications of terahertz spectroscopy and imaging [J]. Trends in Biotechnology, 2016, 34(10): 810-824.

[10] Smolyanskaya O A, Chernomyrdin N V, Konovko A A, et al. Terahertz biophotonics as a tool for studies of dielectric and spectral properties of biological tissues and liquids [J]. Progress in Quantum Electronics, 2018, 62: 1-77.

[11] Gavdush A A, Chernomyrdin N V, Malakhov K M, et al. Terahertz spectroscopy of gelatin-embedded human brain gliomas of different grades: a road toward intraoperative THz diagnosis[J]. Journal of Biomedical Optics, 2019, 24(2): 027001.

[12] Zaytsev K I, Dolganova I N, Chernomyrdin N V, et al. The progress and perspectives of terahertz technology for diagnosis of neoplasms: a review[J]. Journal of Optics, 2020, 22(1): 013001.

[13] Liu X Q, Yao J L, Huang F, et al. Study on detection of penicillin drugs based on terahertz time-domain spectroscopy[J]. Acta Optica Sinica, 2020, 40(6): 0630001.
刘晓庆, 姚嘉丽, 黄凡, 等. 基于太赫兹时域光谱的青霉素类药物检测研究[J]. 光学学报, 2020, 40(6): 0630001.

[14] Graham-Rowe D. Terahertz takes to the stage[J]. Nature Photonics, 2007, 1(2): 75-77.

[15] Mittleman D M, Jacobsen R H, Neelamani R, et

al. Gas sensing using terahertz time-domain spectroscopy[J]. Applied Physics B, 1998, 67(3): 379-390.

[16] Woodward R M, Wallace V P, Arnone D D, et al. Terahertz pulsed imaging of skin cancer in the time and frequency domain [J]. Journal of Biological Physics, 2003, 29(2/3): 257-259.

[17] Federici J F, Schulkin B, Huang F, et al. THz imaging and sensing for security applications: explosives, weapons and drugs[J]. Semiconductor Science and Technology, 2005, 20(7): S266-S280.

[18] van Exter M, Fattinger C, Grischkowsky D. High-brightness terahertz beams characterized with an ultrafast detector [J]. Applied Physics Letters, 1989, 55(4): 337-339.

[19] Kübler C, Huber R, Tübel S, et al. Ultrabroadband detection of multi-terahertz field transients with GaSe electro-optic sensors: approaching the near infrared[J]. Applied Physics Letters, 2004, 85(16): 3360-3362.

[20] Liu K, Xu J Z, Zhang X C. GaSe crystals for broadband terahertz wave detection [J]. Applied Physics Letters, 2004, 85(6): 863-865.

[21] Huber R, Brodschelm A, Tauser F, et al. Generation and field-resolved detection of femtosecond electromagnetic pulses tunable up to 41 THz[J]. Applied Physics Letters, 2000, 76(22): 3191-3193.

[22] Brown E R, McIntosh K A, Nichols K B, et al. Photomixing up to 3.8 THz in low-temperature-grown GaAs[J]. Applied Physics Letters, 1995, 66(3): 285-287.

[23] Wu Q, Zhang X C. Ultrafast electro-optic field sensors [J]. Applied Physics Letters, 1996, 68(12): 1604-1606.

[24] Gu P, Tani M, Kono S, et al. Study of terahertz radiation from InAs and InSb[J]. Journal of Applied Physics, 2002, 91(9): 5533-5537.

[25] Zhang X C, Hu B B, Darrow J T, et al. Generation of femtosecond electromagnetic pulses from semiconductor surfaces [J]. Applied Physics Letters, 1990, 56(11): 1011-1013.

[26] Darrow J T, Hu B B, Zhang X C, et al. Subpicosecond electromagnetic pulses from large-aperture photoconducting antennas [J]. Optics Letters, 1990, 15(6): 323-325.

[27] Guerboukha H, Nallappan K, Skorobogatiy M. Exploiting k-space/frequency duality toward real-time terahertz imaging[J]. Optica, 2018, 5(2): 109-116.

[28] Auston D H. Picosecond optoelectronic switching and gating in silicon[J]. Applied Physics Letters, 1975, 26(3): 101-103.

[29] Mourou G, Stancampiano C V, Blumenthal D. Picosecond microwave pulse generation[J]. Applied Physics Letters, 1981, 38(6): 470-472.

[30] Grischkowsky D, Keiding S, van Exter M, et al. Far-infrared time-domain spectroscopy with terahertz beams of dielectrics and semiconductors [J]. Journal of the Optical Society of America B, 1990, 7(10): 2006-2015.

[31] Auston D H, Cheung K P, Smith P R. Picosecond photoconducting Hertzian dipoles [J]. Applied Physics Letters, 1984, 45(3): 284-286.

[32] Sun F G, Wagoner G A, Bentz D, et al. Measurement of free-space terahertz pulses via long-lifetime photoconductors [C]// LEOS '95. IEEE Lasers and Electro-Optics Society 1995 Annual Meeting, October 30-31, 1995, San Francisco, CA, USA. New York: IEEE Press, 1995: 222-223.

[33] Cai Y, Brener I, Lopata J, et al. Coherent terahertz radiation detection: direct comparison between free-space electro-optic sampling and antenna detection [J]. Applied Physics Letters, 1998, 73(4): 444-446.

[34] Tani M, Lee K S, Zhang X C. Detection of terahertz radiation with low-temperature-grown GaAs-based photoconductive antenna using 1.55 μm probe[J]. Applied Physics Letters, 2000, 77(9): 1396-1398.

[35] Liu T A, Tani M, Nakajima M, et al. Ultrabroadband terahertz field detection by proton-bombarded InP photoconductive antennas [J]. Optics Express, 2004, 12(13): 2954-2959.

[36] O'Hara J F, Zide J, Gossard A C, et al. Enhanced terahertz detection via ErAs: GaAs nanoisland superlattices[J]. Applied Physics Letters, 2006, 88: 251119.

[37] Roehle H, Dietz R J B, Hensel H J, et al. Next generation 1.5 μm terahertz antennas: mesa-structuring of InGaAs/InAlAs photoconductive layers[J]. Optics Express, 2010, 18(3): 2296-2301.

[38] Beck M, Schäfer H, Klatt G, et al. Impulsive terahertz radiation with high electric fields from an amplifier-driven large-area photoconductive antenna [J]. Optics Express, 2010, 18(9): 9251-9257.

[39] Peytavit E, Lepilliet S, Hindle F, et al. Milliwatt-level output power in the sub-terahertz range generated by photomixing in a GaAs photoconductor [J]. Applied Physics Letters, 2011, 99(22): 223508.

[40] Preu S, Mittendorff M, Lu H, et al. 1550 nm ErAs: In(Al)GaAs large area photoconductive emitters[J]. Applied Physics Letters, 2012, 101(10): 101105.

[41] Kostakis I, Saeedkia D, Missous M. Characterization of low temperature InGaAs-InAlAs semiconductor photo mixers at 1.55 μm wavelength illumination for terahertz generation and detection [J]. Journal of Applied Physics, 2012, 111(10): 103105.

[42] Baker C, Gregory I S, Tribe W R, et al. Highly resistive annealed low-temperature-grown InGaAs with sub-500 fs carrier lifetimes [J]. Applied Physics Letters, 2004, 85(21): 4965-4967.

[43] Brorson S D, Zhang J C, Keiding S R. Ultrafast carrier trapping and slow recombination in ion-bombarded silicon on sapphire measured via THz spectroscopy[J]. Applied Physics Letters, 1994, 64(18): 2385-2387.

[44] Piao Z S, Tani M, Sakai K. Carrier dynamics and terahertz radiation in photoconductive antennas[J]. Japanese Journal of Applied Physics, 2000, 39(1): 96-100.

[45] Gupta S, Frankel M Y, Valdmanis J A, et al. Subpicosecond carrier lifetime in GaAs grown by molecular beam epitaxy at low temperatures[J]. Applied Physics Letters, 1991, 59(25): 3276-3278.

[46] Stone M R, Naftaly M, Miles R E, et al. Electrical and radiation characteristics of semilarge photoconductive terahertz emitters [J]. IEEE Transactions on Microwave Theory and Techniques, 2004, 52(10): 2420-2429.

[47] Cai Y, Brener I, Lopata J, et al. Design and performance of singular electric field terahertz photoconducting antennas [J]. Applied Physics Letters, 1997, 71(15): 2076-2078.

[48] Tani M, Matsuura S, Sakai K, et al. Emission characteristics of photoconductive antennas based on low-temperature-grown GaAs and semi-insulating GaAs[J]. Applied Optics, 1997, 36(30): 7853-7859.

[49] Gallagher W J, Chi C C, Duling I N, et al. Subpicosecond optoelectronic study of resistive and superconductive transmission lines [J]. Applied Physics Letters, 1987, 50(6): 350-352.

[50] Zolfagharloo-Koohi M, Neshat M. Antenna efficiency in graphene-based THz photoconductive antennas [C]// 2014 22nd Iranian Conference on Electrical Engineering (ICEE), May 20-22, 2014, Tehran, Iran. New York: IEEE Press, 2014: 1587-1590.

[51] Benicewicz P K, Taylor A J. Scaling of terahertz radiation from large-aperture biased InP photoconductors[J]. Optics Letters, 1993, 18(16): 1332-1334.

[52] Suzuki M, Tonouchi M. Fe-implanted InGaAs terahertz emitters for 1.56 μm wavelength excitation [J]. Applied Physics Letters, 2005, 86(5): 051104.

[53] Pedersen J E, Lyssenko V G, Hvam J M, et al. Ultrafast local field dynamics in photoconductive THz antennas[J]. Applied Physics Letters, 1993, 62(11): 1265-1267.

[54] Hinkov I, Harzendorf G, Kluska S, et al. Generation of terahertz pulsed radiation from photoconductive emitters using 1060 nm laser excitation [C] // 2007 Joint 32nd International Conference on Infrared and Millimeter Waves and the 15th International Conference on Terahertz Electronics, September 2-9, 2007, Cardiff, UK. New York: IEEE Press, 2007: 196-197.

[55] Budiarto E, Margolies J, Jeong S, et al. High-intensity terahertz pulses at 1-kHz repetition rate [J]. IEEE Journal of Quantum Electronics, 1996, 32(10): 1839-1846.

[56] Wu L Z, Zhao G Z, Wang H Y, et al. Terahertz emission of photoconductive antenna under different biased electrical fields [J]. Proceedings of SPIE, 2009, 7512: 75120F.

[57] van Exter M, Grischkowsky D R. Characterization of an optoelectronic terahertz beam system [J]. IEEE Transactions on Microwave Theory and Techniques, 1990, 38(11): 1684-1691.

[58] Jepsen P U, Keiding S R. Radiation patterns from lens-coupled terahertz antennas[J]. Optics Letters, 1995, 20(8): 807-809.

[59] van Rudd J, Mittleman D M. Influence of substrate-lens design in terahertz time-domain spectroscopy [J]. Journal of the Optical Society of America B, 2002, 19(2): 319-329.

[60] Formanek F, Brun M A, Umetsu T, et al. Aspheric silicon lenses for terahertz photoconductive antennas[J]. Applied Physics Letters, 2009, 94(2): 021113.

[61] Globisch B, Dietz R J B, Kohlhaas R B, et al. Iron doped InGaAs: competitive THz emitters and detectors fabricated from the same photoconductor [J]. Journal of Applied Physics, 2017, 121(5): 053102.

[62] Shelby R A, Smith D R, Schultz S. Experimental verification of a negative index of refraction[J]. Science, 2001, 292(5514): 77-79.

[63] Ebbesen T W, Lezec H J, Ghaemi H F, et al. Extraordinary optical transmission through sub-wavelength hole arrays[J]. Nature, 1998, 391(6668): 667-669.

[64] Schurig D, Mock J J, Justice B J, et al. Metamaterial electromagnetic cloak at microwave frequencies[J]. Science, 2006, 314(5801): 977-980.

[65] Ergin T, Stenger N, Brenner P, et al. Three-dimensional invisibility cloak at optical wavelengths[J]. Science, 2010, 328(5976): 337-339.

[66] Cong L Q, Singh R. Symmetry-protected dual bound states in the continuum in metamaterials[J]. Advanced Optical Materials, 2019: 1900383.

[67] Koshelev K, Lepeshov S, Liu M K, et al. Asymmetric metasurfaces with high-*Q* resonances governed by bound states in the continuum[J]. Physical Review Letters, 2018, 121(19): 193903.

[68] Landy N I, Sajuyigbe S, Mock J J, et al. Perfect metamaterial absorber[J]. Physical Review Letters, 2008, 100(20): 207402.

[69] Zhang Y, Li T, Chen Q, et al. Independently tunable dual-band perfect absorber based on graphene at mid-infrared frequencies[J]. Scientific Reports, 2015, 5: 18463.

[70] Cui Z J, Wang Y, Zhu D Y, et al. Perfect absorption conditions and absorption characteristics of terahertz metamaterial absorber[J]. Chinese Journal of Lasers, 2019, 46(6): 0614023.
崔子健, 王玥, 朱冬颖, 等. 太赫兹超材料吸收器的完美吸收条件与吸收特性[J]. 中国激光, 2019, 46(6): 0614023.

[71] Pendry J B. Negative refraction makes a perfect lens[J]. Review Letters, 2000, 85(18): 3966-3969.

[72] Fang N, Lee H, Sun C, et al. Sub-diffraction-limited optical imaging with a silver superlens[J]. Science, 2005, 308(5721): 534-537.

[73] Zhang S, Genov D A, Wang Y, et al. Plasmon-induced transparency in metamaterials[J]. Physical Review Letters, 2008, 101(4): 047401.

[74] Zhang M, Yan F P, Du X M, et al. Design and analysis of electromagnetically induced transparency in THz multiband[J]. Chinese Journal of Lasers, 2021, 48(3): 0314001.
张敏, 延凤平, 杜雪梅, 等. 太赫兹多波段的电磁诱导透明设计与分析[J]. 中国激光, 2021, 48(3): 0314001.

[75] Liu N, Langguth L, Weiss T, et al. Plasmonic analogue of electromagnetically induced transparency at the Drude damping limit[J]. Nature Materials, 2009, 8(9): 758-762.

[76] Liu X, Deng J H, Jin M K, et al. Cassegrain metasurface for generation of orbital angular momentum of light[J]. Applied Physics Letters, 2019, 115(22): 221102.

[77] Ren H R, Briere G, Fang X Y, et al. Metasurface orbital angular momentum holography[J]. Nature Communications, 2019, 10(1): 2986.

[78] Park D, Jeong K, Maeng I, et al. Ultrafast photo-response by surface state-mediated optical transitions in topological insulator Bi_2Te_3 nanowire[J]. Advanced Optical Materials, 2019, 7(19): 1900621.

[79] Xie F J, Lian Z, Zhang S, et al. Reversible engineering of topological insulator surface state conductivity through optical excitation[J]. Nanotechnology, 2021, 32(17): 17LT01.

[80] Huang S Y, Xu X F. Optical chirality detection using a topological insulator transistor[J]. Advanced Optical Materials, 2021, 9(10): 2002210.

[81] Cong L Q, Xu N N, Han J G, et al. A tunable dispersion-free terahertz metadevice with pancharatnam-berry-phase-enabled modulation and polarization control[J]. Advanced Materials, 2015, 27(42): 6630-6636.

[82] Kenney M, Li S X, Zhang X Q, et al. Pancharatnam-berry phase induced spin-selective transmission in herringbone dielectric metamaterials[J]. Advanced Materials, 2016, 28(43): 9567-9572.

[83] Schurig D, Mock J J, Smith D R. Electric-field-coupled resonators for negative permittivity metamaterials[J]. Applied Physics Letters, 2006, 88(4): 041109.

[84] O'Hara J F, Chen H T, Taylor A J, et al. Split-ring resonator enhanced terahertz antenna[C]// Nonlinear Optics: Materials, Fundamentals and Applications 2007, July 30, 2007, Kona, Hawaii, United States. Washington, D. C.: OSA, 2007: TuB2.

[85] Atwater H A, Polman A. Plasmonics for improved photovoltaic devices[J]. Nature Materials, 2010, 9(3): 205-213.

[86] Chettiar U K, Garcia R F, Maier S A, et al. Enhancement of radiation from dielectric waveguides using resonant plasmonic coreshells[J]. Optics Express, 2012, 20(14): 16104-16112.

[87] Genevet P, Tetienne J P, Gatzogiannis E, et al. Large enhancement of nonlinear optical phenomena by plasmonic nanocavity gratings[J]. Nano Letters, 2010, 10(12): 4880-4883.

[88] Knight M W, Grady N K, Bardhan R, et al. Nanoparticle-mediated coupling of light into a nanowire[J]. Nano Letters, 2007, 7(8): 2346-2350.

[89] Grady N K, Knight M W, Bardhan R, et al. Optically-driven collapse of a plasmonic nanogap self-monitored by optical frequency mixing[J]. Nano Letters, 2010, 10(4): 1522-1528.

[90] Matsui T, Agrawal A, Nahata A, et al. Transmission resonances through aperiodic arrays of subwavelength apertures[J]. Nature, 2007, 446(7135): 517-521.

[91] Soukoulis C M, Wegener M. Past achievements and future challenges in the development of three-dimensional photonic metamaterials[J]. Nature Photonics, 2011, 5(9): 523-530.

[92] Thompson R J, Siday T, Glass S, et al. Optically thin hybrid cavity for terahertz photo-conductive detectors[J]. Applied Physics Letters, 2017, 110(4): 041105.

[93] Cao Y H, Liu Z Y, Minin O V, et al. Deep subwavelength-scale light focusing and confinement in nanohole-structured mesoscale dielectric spheres[J]. Nanomaterials, 2019, 9(2): 186.

[94] Moitra P, Slovick B A, Li W, et al. Large-scale all-dielectric metamaterial perfect reflectors[J]. ACS Photonics, 2015, 2(6): 692-698.

[95] Jahani S, Jacob Z. All-dielectric metamaterials[J]. Nature Nanotechnology, 2016, 11(1): 23-36.

[96] Genet C, Ebbesen T W. Light in tiny holes[J]. Nature, 2007, 445(7123): 39-46.

[97] Park S G, Jin K H, Yi M, et al. Enhancement of terahertz pulse emission by optical nanoantenna[J]. ACS Nano, 2012, 6(3): 2026-2031.

[98] Park S G, Choi Y, Oh Y J, et al. Terahertz photoconductive antenna with metal nanoislands[J]. Optics Express, 2012, 20(23): 25530-25535.

[99] Jooshesh A, Smith L, Masnadi-Shirazi M, et al. Nanoplasmonics enhanced terahertz sources[J]. Optics Express, 2014, 22(23): 27992-28001.

[100] Jooshesh A, Fesharaki F, Bahrami-Yekta V, et al. Plasmon-enhanced LT-GaAs/AlAs heterostructure photoconductive antennas for sub-bandgap terahertz generation[J]. Optics Express, 2017, 25(18): 22140-22148.

[101] Fesharaki F, Jooshesh A, Bahrami-Yekta V, et al. Plasmonic antireflection coating for photoconductive terahertz generation[J]. ACS Photonics, 2017, 4(6): 1350-1354.

[102] Jooshesh A, Bahrami-Yekta V, Zhang J, et al. Plasmon-enhanced below bandgap photoconductive terahertz generation and detection[J]. Nano Letters, 2015, 15(12): 8306-8310.

[103] Rämer J M, Ospald F, von Freymann G, et al. Generation and detection of terahertz radiation up to 4.5 THz by low-temperature grown GaAs photoconductive antennas excited at 1560 nm[J]. Applied Physics Letters, 2013, 103(2): 021119.

[104] Thompson R J, Siday T, Glass S, et al. Optically thin hybrid cavity for terahertz photo-conductive detectors[J]. Applied Physics Letters, 2017, 110(4): 041105.

[105] Mitrofanov O, Brener I, Luk T S, et al. Photoconductive terahertz near-field detector with a hybrid nanoantenna array cavity[J]. ACS Photonics, 2015, 2(12): 1763-1768.

[106] Bashirpour M, Ghorbani S, Kolahdouz M, et al. Significant performance improvement of a terahertz photoconductive antenna using a hybrid structure[J]. RSC Advances, 2017, 7(83): 53010-53017.

[107] Ghorbani S, Bashirpour M, Poursafar J, et al. Thin film tandem nanoplasmonic photoconductive antenna for high performance terahertz detection[J]. Superlattices and Microstructures, 2018, 120: 598-604.

[108] Burford N M, Evans M J, El-Shenawee M O. Plasmonic nanodisk thin-film terahertz photoconductive antenna[J]. IEEE Transactions on Terahertz Science and Technology, 2018, 8(2): 237-247.

[109] Gric T, Gorodetsky A, Trofimov A, et al. Tunable plasmonic properties and absorption enhancement in terahertz photoconductive antenna based on optimized plasmonic nanostructures[J]. Journal of Infrared, Millimeter, and Terahertz Waves, 2018, 39(10): 1028-1038.

[110] Lepeshov S, Gorodetsky A, Krasnok A, et al. Boosting terahertz photoconductive antenna performance with optimised plasmonic nanostructures[J]. Scientific Reports, 2018, 8(1): 6624.

[111] Bhattacharya A, Ghindani D, Prabhu S S. Enhanced terahertz emission bandwidth from photoconductive antenna by manipulating carrier dynamics of semiconducting substrate with embedded plasmonic metasurface[J]. Optics Express, 2019, 27(21): 30272-30279.

[112] Bashirpour M, Poursafar J, Kolahdouz M, et al. Terahertz radiation enhancement in dipole photoconductive antenna on LT-GaAs using a gold plasmonic nanodisk array[J]. Optics & Laser Technology, 2019, 120: 105726.

[113] Murakami H, Takarada T, Tonouchi M. Low-temperature GaAs-based plasmonic photoconductive

terahertz detector with Au nano-islands [J]. Photonics Research, 2020, 8(9): 1448-1456.

[114] Jiang R, Cheng S, Li Q Y, et al. Terahertz radiation enhancement based on LT-GaAs by optimized plasmonic nanostructure [J]. Laser Physics, 2021, 31(3): 036203.

[115] Tong J C, Suo F, Zhang T N, et al. Plasmonic semiconductor nanogroove array enhanced broad spectral band millimetre and terahertz wave detection[J]. Light: Science & Applications, 2021, 10(1): 58.

[116] Heshmat B, Pahlevaninezhad H, Pang Y J, et al. Nanoplasmonic terahertz photoconductive switch on GaAs[J]. Nano Letters, 2012, 12(12): 6255-6259.

[117] Berry C W, Wang N, Hashemi M R, et al. Significant performance enhancement in photoconductive terahertz optoelectronics by incorporating plasmonic contact electrodes [J]. Nature Communications, 2013, 4: 1622.

[118] Yang S H, Hashemi M R, Berry C W, et al. 7.5% optical-to-terahertz conversion efficiency offered by photoconductive emitters with three-dimensional plasmonic contact electrodes[J]. IEEE Transactions on Terahertz Science and Technology, 2014, 4(5): 575-581.

[119] Moon K, Lee I M, Shin J H, et al. Bias field tailored plasmonic nano-electrode for high-power terahertz photonic devices [J]. Scientific Reports, 2015, 5: 13817.

[120] Moon K, Lee E S, Lee I M, et al. Photo-conductive detection of continuous THz waves via manipulated ultrafast process in nanostructures [J]. Applied Physics Letters, 2018, 112(3): 031102.

[121] Singh A, Welsch M, Winnerl S, et al. Improved electrode design for interdigitated large-area photoconductive terahertz emitters [J]. Optics Express, 2019, 27(9): 13108-13115.

[122] Li M D, Lu G Z. Application of sub-wavelength grating electrodes in photo conductive antennas[J]. Plasmonics, 2019, 14(4): 807-813.

[123] Lavrukhin D V, Yachmenev A E, Glinskiy I, et al. Terahertz photoconductive emitter with dielectric-embedded high-aspect-ratio plasmonic grating for operation with low-power optical pumps[C]//2019 International Workshop on Antenna Technology (IWAT), March 3-6, 2019, Miami, FL, USA. New York: IEEE Press, 2019: 21-24.

[124] Khorshidi M, Zafari S, Dadashzadeh G. Increase in terahertz radiation power of plasmonic photoconductive antennas by embedding buried three-stepped rods in electrodes [J]. Optics Express, 2019, 27(16): 22327-22338.

[125] Singh A, Welsch M, Winnerl S, et al. Non-plasmonic improvement in photoconductive THz emitters using nano- and micro-structured electrodes [J]. Optics Express, 2020, 28(24): 35490-35497.

[126] Berry C W, Hashemi M R, Jarrahi M. Generation of high power pulsed terahertz radiation using a plasmonic photoconductive emitter array with logarithmic spiral antennas [J]. Applied Physics Letters, 2014, 104(8): 081122.

[127] Yardimci N T, Yang S H, Berry C W, et al. High-power terahertz generation using large-area plasmonic photoconductive emitters [J]. IEEE Transactions on Terahertz Science and Technology, 2015, 5(2): 223-229.

[128] Yardimci N T, Cakmakyapan S, Hemmati S, et al. Significant efficiency enhancement in photoconductive terahertz emitters through three-dimensional light confinement [C]// 2017 IEEE MTT-S International Microwave Symposium (IMS), June 4-9, 2017, Honolulu, HI, USA. New York: IEEE Press, 2017: 435-438.

[129] Yardimci N T, Lu H, Jarrahi M. High power telecommunication-compatible photoconductive terahertz emitters based on plasmonic nano-antenna arrays [J]. Applied Physics Letters, 2016, 109(19): 191103.

[130] Yardimci N T, Jarrahi M. High sensitivity terahertz detection through large-area plasmonic nano-antenna arrays[J]. Scientific Reports, 2017, 7: 42667.

[131] Yardimci N T, Turan D, Cakmakyapan S, et al. A high-responsivity and broadband photoconductive terahertz detector based on a plasmonic nanocavity [J]. Applied Physics Letters, 2018, 113(25): 251102.

[132] Turan D, Yardimci N T, Jarrahi M. Plasmonics-enhanced photoconductive terahertz detector pumped by Ytterbium-doped fiber laser[J]. Optics Express, 2020, 28(3): 3835-3845.

[133] Lu P K, Turan D, Jarrahi M. High-sensitivity telecommunication-compatible photoconductive terahertz detection through carrier transit time reduction [J]. Optics Express, 2020, 28(18): 26324-26335.

[134] Balow A M, Khatir M, Amiri N. Terahertz detection using large-area plasmonic nano-antenna arrays based on stepped strips [J]. Optik, 2021, 228: 165886.

[135] Tanoto H, Teng J H, Wu Q Y, et al. Nano-antenna in a photoconductive photomixer for highly efficient continuous wave terahertz emission [J].

Scientific Reports, 2013, 3: 2824.

[136] Berry C W, Hashemi M R, Preu S, et al. Plasmonics enhanced photomixing for generating quasi-continuous-wave frequency-tunable terahertz radiation[J]. Optics Letters, 2014, 39(15): 4522-4524.

[137] Berry C W, Hashemi M R, Preu S, et al. High power terahertz generation using 1550 nm plasmonic photomixers[J]. Applied Physics Letters, 2014, 105(1): 011121.

[138] Yang S H, Jarrahi M. Frequency-tunable continuous-wave terahertz sources based on GaAs plasmonic photomixers [J]. Applied Physics Letters, 2015, 107(13): 131111.

[139] Yang S H, Jarrahi M. Spectral characteristics of terahertz radiation from plasmonic photomixers[J]. Optics Express, 2015, 23(22): 28522-28530.

[140] Khorshidi M, Dadashzadeh G. Dielectric structure with periodic strips for increasing radiation power of photoconductive antennas: theoretical analysis[J]. Journal of Infrared, Millimeter, and Terahertz Waves, 2017, 38(5): 609-629.

[141] Mitrofanov O, Siday T, Thompson R J, et al. Efficient photoconductive terahertz detector with all-dielectric optical metasurface[J]. APL Photonics, 2018, 3(5): 051703.

[142] Siday T, Vabishchevich P P, Hale L, et al. Terahertz detection with perfectly-absorbing photoconductive metasurface [J]. Nano Letters, 2019, 19(5): 2888-2896.

[143] Wang K M, Gu J Q, Shi W Q, et al. All-dielectric nanograting for increasing terahertz radiation power of photoconductive antennas[J]. Optics Express, 2020, 28(13): 19144-19151.

[144] Takano K, Chiyoda Y, Nishida T, et al. Optical switching of terahertz radiation from meta-atom-loaded photoconductive antennas [J]. Applied Physics Letters, 2011, 99(16): 161114.

[145] Liu S C, Shou X, Nahata A. Coherent detection of multiband terahertz radiation using a surface plasmon-polariton based photoconductive antenna [J]. IEEE Transactions on Terahertz Science and Technology, 2011, 1(2): 412-415.

[146] Shi X C, Wang K M, Gu J Q, et al. Photoconductive meta-antenna enabling terahertz amplitude spectrum manipulation [J]. Advanced Photonics Research, 2021, 2(1): 2000036.

[147] Zhao Z Y, Zheng X B, Ollmann Z, et al. Terahertz selective emission enhancement from a metasurface-coupled photoconductive emitter in quasi-near-field zone[J]. Plasmonics, 2020, 15(1): 263-269.

[148] Hu D, Wang X K, Feng S F, et al. Ultrathin terahertz planar elements [J]. Advanced Optical Materials, 2013, 1(2): 186-191.

[149] Jiang X Y, Ye J S, He J W, et al. An ultrathin terahertz lens with axial long focal depth based on metasurfaces[J]. Optics Express, 2013, 21(24): 30030-30038.

[150] Wang Q, Zhang X Q, Xu Y H, et al. A broadband metasurface-based terahertz flat-lens array [J]. Advanced Optical Materials, 2015, 3(6): 779-785.

[151] Wang S, Wang X K, Kan Q, et al. Spin-selected focusing and imaging based on metasurface lens[J]. Optics Express, 2015, 23(20): 26434-26441.

[152] Luo J, Yu H L, Song M W, et al. Highly efficient wavefront manipulation in terahertz based on plasmonic gradient metasurfaces [J]. Optics Letters, 2014, 39(8): 2229-2231.

[153] Yang Q L, Gu J Q, Wang D Y, et al. Efficient flat metasurface lens for terahertz imaging[J]. Optics Express, 2014, 22(21): 25931-25939.

[154] Yang Q L, Gu J Q, Xu Y H, et al. Broadband and robust metalens with nonlinear phase profiles for efficient terahertz wave control [J]. Advanced Optical Materials, 2017, 5(10): 1601084.

[155] Yu Q, Gu J Q, Yang Q L, et al. All-dielectric meta-lens designed for photoconductive terahertz antennas [J]. IEEE Photonics Journal, 2017, 9(4): 1-9.

[156] Jia D, Tian Y, Ma W, et al. Transmissive terahertz metalens with full phase control based on a dielectric metasurface[J]. Optics Letters, 2017, 42(21): 4494-4497.

[157] Jiang X, Chen H, Li Z, et al. All-dielectric metalens for terahertz wave imaging [J]. Optics Express, 2018, 26(11): 14132-14142.

[158] Cheng Q Q, Ma M L, Yu D, et al. Broadband achromatic metalens in terahertz regime[J]. Science Bulletin, 2019, 64(20): 1525-1531.

[159] Gao Y F, Gu J Q, Jia R D, et al. Polarization independent achromatic meta-lens designed for the terahertz domain[J]. Frontiers in Physics, 2020, 8: 606693.

[160] Fakhar B H, Ghazialsharif M, Abrishamian M S. Graphene hybrid waveguide stimulation using a photoconductive terahertz generator [J]. Optics Letters, 2020, 45(8): 2407-2410.

[161] Doha M H, Batista J I S, Rawwagah A F, et al. Integration of multi-layer black phosphorus into photoconductive antennas for THz emission [J]. Journal of Applied Physics, 2020, 128(6): 063104.

[162] Zhou Y X, Huang Y Y, Jin Y P, et al. Terahertz properties of graphene and graphene-based terahertz

devices[J]. Chinese Journal of Lasers, 2019, 46(6): 0614011.
周译玄, 黄媛媛, 靳延平, 等. 石墨烯太赫兹波段性质及石墨烯基太赫兹器件[J]. 中国激光, 2019, 46(6): 0614011.
[163] Kang M, Feng T H, Wang H T, et al. Wave front engineering from an array of thin aperture antennas [J]. Optics Express, 2012, 20(14): 15882-15890.
[164] Sun S L, He Q, Xiao S Y, et al. Gradient-index meta-surfaces as a bridge linking propagating waves and surface waves[J]. Nature Materials, 2012, 11(5): 426-431.
[165] Yu N, Genevet P, Kats M A, et al. Light propagation with phase discontinuities: generalized laws of reflection and refraction[J]. Science, 2011, 334(6054): 333-337.

Metamaterials-Based Terahertz Photoconductive Antennas

Gu Jianqiang[1*], Wang Kemeng[1], Xu Yi[1], Ouyang Chunmei[1], Tian Zhen[1], Han Jiaguang[1], Zhang Weili[2]

[1] *Center for THz Waves, College of Precision Instrument and Optoelectronics Engineering, Tianjin University, Tianjin* 300072, *China*;

[2] *School of Electrical and Computer Engineering, Oklahoma State University, Stillwater, Oklahoma* 74078, *America*

Abstract

Significance As the cornerstone of terahertz technologies, terahertz radiation sources and detectors have attracted lots of attention. The research on terahertz sources and detectors has run through the entire development of terahertz technologies. In recent years, terahertz technologies have become more closely integrated with other disciplines, which puts forward higher requirements on the sources and the detectors. As the most typical terahertz transmitter and receiver, an photoconductive antennas (PCA) is widely used in laboratories and commercial terahertz systems due to its low request on pump power and compatibility with fiber technologies. The current commercial photoconductive antenna can meet the needs of spectral analysis of thin and low-absorption samples. However, compared with those of solid-state terahertz sources, the power of a PCA is at least two orders of lower. While compared with those of low-temperature thermal detectors, the sensitivity of a detection antennas is also insufficient, not to mention its low-pass filtering effect that is adverse to the detection of high-frequency terahertz waves. Thus, developing a high-performance PCA is an important issue to promote terahertz technologies.

Surprisingly, the emergence of metamaterials sheds light on the development of advanced PCAs. With the extremely high degree of design freedom, metamaterials have become one of the mostly concerned artificial electromagnetic media platforms. In the past 20 years, metamaterials have attracted many outstanding researchers in electromagnetics, optics, acoustics, and thermodynamics. Numerous novel functions have been realized one after another, such as negative refractive index, electromagnetic cloak, bounded state in the continuum, perfect absorption, meta-lens, plasmon induced transparency, optical orbital angular momentum coupling, and optical topological insulator. The unique properties of metamaterials can also be used to improve the performance of photoconductive antennas. This review systematically introduces the research works of efficient photoconductive antennas based on metal and dielectric metamaterials. The germination, development and broad application prospects of metamaterial-assisted photoconductive antennas are elaborated. The novel methods based on metamaterials have greatly promoted the development of photoconductive antennas and we hope this review could bring in more researchers in this new direction.

Progress We have classified the reported metamaterial-assisted photoconductive antennas into two categories. The first one is to enhance the interaction strength between the femtosecond laser pump and the substrate by using nano-scale metal or dielectric metamaterials. Metamaterials can manipulate the amplitude, phase and polarization of an electromagnetic wave with a high degree of freedom. In general, surface plasmons excited on metallic metamaterials have excellent field localization, which can tightly confine the light field near the structure, thereby enhancing the interaction between the photoconductive substrate and the incident light field. But so far, most metallic metamaterials have been severely affected by high ohmic losses, especially in the visible and near-infrared domains.

In recent years, it has been found that dielectric metamaterials can also form field localization and have low absorption loss. Such metamaterials are generally composed of dielectric microcavities with high refractive index, which support rich electric field resonance modes. This review summarized the works which enhance the absorption of the pump light by the metallic or dielectric nanostructures, thus greatly improve the light-terahertz conversion efficiency and the detection sensitivity (as shown in Figs. 2, 6 and 7). In addition to being integrated in the antenna gap, the metallic nano-metamaterials can also be directly used as the electrode of the antenna, which changes the electrode shape. By this method, the transport time for the carrier to the electrode is reduced, and the performance of the terahertz photoconductive antenna is improved (as shown in Fig. 3). Furthermore, as shown in Fig. 4, constructing an antenna array integrated with nano-electrodes can increase the upper limit of pump power, thereby avoiding the saturation effect of the femtosecond laser pump. This method can increase the terahertz power by more than one order of magnitude. Besides, we also mention that metamaterials can also improve the performance of photomixers, which are more important in the fields of terahertz communication and imaging (as shown in Fig. 5).

The second category is to design micron-scale metallic or dielectric metamaterials for directly manipulating terahertz waves. Designing a micron structure near the antenna electrode can effectively manipulate the spectral characteristics of the radiated terahertz wave, as shown in Figs. 8 and 9. Another way to manipulate the radiated terahertz pulse is to construct an all-dielectric meta-lens sticked to the photoconductive substrate for replacing the hyper-semispherical silicon lens and collimating the terahertz wave to a parallel beam (as shown in Fig. 10).

Conclusion and Prospect This review introduces a series of terahertz photoconductive antennas integrated with metamaterials. Their excellent properties and novel functions may bring a huge application potential, which have greatly promoted the development of photoconductive antennas.

The methodology reviewed here is still in its early stage. We believe that more metamaterials with novel functions will be applied in the future. Besides, the introduction of new materials, for example two-dimensional materials such as graphene and black phosphorus, may cause fundamental changes in the design of photoconductive antennas. Another possible research direction is to integrate phase gradient metamaterials based on the generalized Snell's law for manipulating the wavefront of photoconductive antenna emitted terahertz wave. Besides, considering the significance of photomixers to terahertz communications, using new metamaterials to realize an active control of photomixers becomes more and more important.

In short, the novel antennas shown in this review have a great application potential in terahertz technologies, which are expected to fundamentally promote the development of photoconductive antennas and significantly advance the performance of terahertz photoconductive devices.

Key words terahertz technology; ultrafast optics; photoconductive antenna; metamaterials; local field enhancement; terahertz radiation; terahertz detection

OCIS codes 320.7080; 160.3918; 250.5403; 040.2235